Available online at www.sciencedirect.com
SCIENCE DIRECT®
Journal of Sound and Vibration 295 (2006) 939–963
JOURNAL OF SOUND AND VIBRATION
www.elsevier.com/locate/jsvi

A split-frequency harmonic balance method for nonlinear oscillators with multi-harmonic forcing

J.F. Dunne*, P. Hayward

Department of Engineering and Design, School of Science and Technology, The University of Sussex, Falmer, Brighton, BN1 9QT, UK

Received 18 February 2005; received in revised form 11 November 2005; accepted 30 January 2006
Available online 29 March 2006

Abstract

A new harmonic balance method (HBM) is presented for accurately computing the periodic responses of a nonlinear sdof oscillator with multi-harmonic forcing and non-expansible nonlinearities. The presence of multi-harmonic forcing requires a large number of solution harmonics with a substantial increase in computational demand for either the conventional or the incremental HBM. In this method, the oscillator equation-error is first defined in terms of two functions (originally proposed for obtaining free-vibration periods in: R.E. Mickens, Iteration procedure for determining approximate solutions to nonlinear oscillator equations, *Journal of Sound and Vibration* 116 (1987) 185–187; and more recently: R.E. Mickens, A Generalised iteration procedure for calculating approximations to periodic solutions of "truly nonlinear oscillations", *Journal of Sound and Vibration* 287 (2005) 1045–1051). A Fourier series solution is assumed, in which the total number of harmonics is fixed by the chosen discrete-time interval—this series is split into two partial sums nominally associated with either low-frequency or high-frequency harmonics. By exploiting a convergence property of the equation-error functions, the total solution is obtained in a new iterative scheme in which the low-frequency components are computed via a conventional HBM using a small number of algebraic equations, whereas the high frequency components are obtained in a separate step by updating. By gradually increasing the number of harmonics in the low-frequency group, the equation-error can be progressively reduced. Efficient use is made of FFT-based algebraic equation generation which allows an important class of non-expansible nonlinearities to be handled. The proposed method is tested on a Duffing-type oscillator, and an oscillator with a non-expansible 7th power stiffness term, where in both cases up to 24 component multi-harmonic forcing is applied. As a comparison, a conventional HBM is also used on the Duffing model in which the algebraic equations are generated in symbolic form to totally avoid errors from entering the formulation through complicated expansion of the cubic stiffness term (as in: I. Senjanović, Harmonic analysis of nonlinear oscillations of cubic dynamical systems, *Journal of Ship Research* 38 (3) (1994) 225–238; and in: A. Raghothama, S. Narayanan, Periodic response and chaos in nonlinear systems with parametric excitation and time delay, *Nonlinear dynamics* 27 (2002) 341–365). The paper shows that in obtaining period-1 solutions, the computational accuracy and efficiency of the proposed method is very good.

*Corresponding author. Tel.: +44 1273 606755x2570; fax: +44 1273 678399.
E-mail address: j.f.dunne@sussex.ac.uk (J.F. Dunne).

0022-460X/$ - see front matter © 2006 Elsevier Ltd. All rights reserved.
doi:10.1016/j.jsv.2006.01.050

1. Introduction

Nonlinear oscillator models arise in many areas of physics and engineering and are important in mechanical dynamics for accurate prediction of forced motion. An important class of externally excited sdof oscillators are those with non-expansible nonlinearities and periodic multi-harmonic forcing, rather than just single-harmonic excitation. Non-expansible nonlinearities are understood to mean those functions which cannot in practice be expanded into explicit Fourier series when the argument of the function is also expressed as a Fourier series. Quadratic and cubic terms are examples of expansible functions but 5th and higher powers are not. Many investigations have focused on single-harmonic forcing of the Duffing oscillator, to predict motion at the driving frequency, as well as sub- and super-harmonic resonances. Other studies have gone further, using stability analysis to find bifurcations, period-doubling, jumping phenomena, and transition conditions from periodic to chaotic behaviour. Since this multi-valued behaviour is highly sensitive to initial conditions, time-domain integration techniques are of limited value, except for generating stable solutions using known steady-state initial conditions. Alternative approximate approaches, such as the perturbation method [1], multiple scales [2], and the harmonic balance method (HBM) [3–21] have been developed to study forced periodic motion. Of these, the HBM is by far the most widely used because it can handle strongly nonlinear behaviour; it can be extended to MDOF systems; and because the approximation error can in principle, be reduced to any level.

This paper focuses on a new form of HBM to address multi-harmonic forcing and non-expansible nonlinearities. The HBM has already received considerable attention over the past two decades to address a number of general questions [3–12], and specific applications include studies on flow-induced vibration [13], ship rolling motion [14–16], rotor dynamics [17–19], thermally coupled beam vibrations [20], and gear-train dynamics [21]. The HBM has also been used in electro-dynamic applications to study communication circuits [22], and magnetic-field saturation [23]. Multi-harmonic forcing arises for example, in rolling contact pulse-loading on machines, through gas pressure variation in IC engines and gas-turbine blade movement past fixed nozzles (where in linear models, superposition allows individual harmonics to be treated separately as 'engine order' excitation). Other sources include out-of-balance forces in mechanisms and multi-shaft rotors (with rational speed ratios), torque transmission through couplings, and from wave loading on offshore and ship structures in regular wave-tank tests. A number of studies have considered multi-harmonic forcing with quadratic and cubic stiffness. For example in Ref. [20], two forcing harmonics were used, and up to 32 harmonics in the response; and in Ref. [14], a total of 20 excitation harmonics were used, and up to 134 harmonics in the response; elsewhere in Ref. [22], three input harmonics justified 30 response harmonics; and in Ref. [23], a square wave input was modelled with 15 harmonics, with the same number in the response. The inclusion of more harmonics in the forcing function makes no difference to the HBM formulation since this depends on whether the nonlinearity is expansible. But the need to substantially increase the number of solution harmonics compounds the HBM formulation and the computational effort, especially for non-expansible nonlinearities [16].

To appreciate these combined factors, consider the three main tasks involved in generating a periodic solution using the HBM. First an approximate solution is assumed in the form of a truncated Fourier series with undetermined coefficients. Next, the assumed solution is manipulated in the model, using appropriate identities to generate a vector of algebraic equations for the coefficients. Finally the algebraic equations are solved, either in direct form, as a minimisation problem, or as a series of linear iterations using the incremental harmonic balance method (IHBM) [4–6]. An accurate HBM solution can then be used in a continuation scheme to obtain a neighbourhood solution for a small parameter change using either the IHBM [20] or Arc Length Continuation [17]. Regarding the number of solution harmonics needed, with single harmonic forcing, prior knowledge of an application can allow a substantial reduction. On a rotor problem for example [17], four response harmonics were found to give a similar qualitative solution as using 32 harmonics. But similar economy is not generally possible with multi-harmonic forcing. And with regard to the feasibility of constructing the algebraic equations, an explicit system can only be generated for quadratic and cubic terms [12]. For higher powers and more general types of nonlinearity, conventional algebraic manipulation is simply not feasible although attempts can be made using symbolic computation.

When explicit algebraic equations cannot be generated via conventional or symbolic manipulation, a different approach is needed. Use of the FFT offers an alternative approach by enabling implicit generation of the algebraic equations in temporary numerical form (i.e. made available when needed). This allows much more complex types of nonlinearity to be handled. The problem then however, switches to the computational cost and accuracy of solving the system of algebraic equations expressed in numerical form. For multi-harmonic forcing, where a potentially huge number of response harmonics are needed, the computational cost of FFT generation is unacceptable. A method is therefore needed that can accurately and efficiently handle non-expansible nonlinearities with large numbers of solution harmonics.

In this paper, a new HBM method is presented which utilises FFT-based algebraic equation generation allowing non-expansible nonlinearities to be handled. First the oscillator equation-error is defined in terms of two functions [24–26]. Then the assumed Fourier series solution is split (in a novel way) into two partial sums, nominally associated with either low-frequency or high-frequency harmonics. By exploiting a convergence property of the equation-error functions, the total solution is obtained in a new iterative scheme, in which the low-frequency components are obtained via a conventional HBM involving only a small number of algebraic equations, whereas the high frequency components are obtained in a separate step by updating. The objective of the paper is to establish the accuracy and efficiency of the method in computing period-1 responses for oscillators with varying degrees of multi-harmonic forcing and with non-expansible nonlinearity. For application to the Duffing oscillator with multi-harmonic excitation, the proposed method is compared with a fully conventional HBM in which the algebraic equations are generated using symbolic computation. This is done to totally avoid errors from entering the algebraic equation formulation, and thus to establish objective limitations in the use of a symbolic computing technique with a fully conventional HBM.

2. An iterative split-frequency harmonic balance method

The basis of this new split frequency harmonic balance method (SF-HBM) is now fully developed for a class of sdof oscillators with arbitrary periodic forcing expressed as a finite Fourier series. The overall approach first involves re-defining the oscillator model in terms of two functions (originally proposed by Mickens [24,26] for iterative approximation of the free-vibration period of an oscillator). The response harmonics are then assumed in the form of a Fourier series which is split into two groups: one group nominally associated with 'low' frequency harmonics, the other group nominally associated with 'high' frequency harmonics. This splitting of the harmonics leads to an iterative scheme (different from that proposed by Mickens [26]) in which an HBM is used to find the coefficients associated with the low frequency response harmonics. The high-frequency harmonics are updated using the low-frequency harmonics, which are in turn, revised iteratively. Certain nonlinear operations are expediently performed using a discrete-time formulation, in which an FFT is efficiently used. In particular, an FFT is used to do the following related things: (i) to obtain individual derivatives in the model; (ii) to form the equation error; (iii) to construct the HBM equations; and finally (iv) to generate a set of coefficients needed to update the high-frequency harmonics. The HBM equations, which remain small in number, can then be solved using a conventional least square error solver. By starting-off with just one low-frequency harmonic, and gradually adding more terms, this formulation allows the equation error to be iteratively reduced. But the total number of harmonics in the solution remains fixed, as decided by the discrete time interval. This splitting of response harmonics into these two groups, and the use of the FFT to form the low frequency HBM equations, makes it possible for the method to efficiently handle multi-harmonic forcing and non-expansible nonlinearities.

Now the class of sdof oscillator models is assumed in the form:

$$\ddot{y} + F(y, \dot{y}) = f(t) \tag{1}$$

with excitation $f(t)$ is assumed to be periodic and represented in the form of Fourier series:

$$f(t) = \sum_{k=-m}^{m} C_k e^{j\Omega_k t}, \tag{2}$$

where $\Omega_k = k\Omega_1$. The function $F(y, \dot{y})$ in Eq. (1) need not be a polynomial function of its arguments, however the existence of a periodic solution must be assumed from the outset (as for the success of the HBM in

general). If the function $F(y,\dot{y})$ is of acceptable form to obtain a periodic solution $y(t)$ (with fundamental frequency Ω_1), then two additional conditions must be imposed on $F(y,\dot{y})$: (i) $F(y,\dot{y})$ must have a Fourier series representation with fundamental frequency Ω_1; and (ii) $F(y,\dot{y})$ should not contain jump discontinuities, since an unacceptable discrete-time interval might otherwise be needed to meet the Nyquist criterion. This excludes for example, ideal nonlinearities that can arise in impact problems. Also, the assumed solution is limited to the same discrete frequencies as defined in the periodic excitation. The solution method proposed here does not exclude the possibility that the fundamental excitation frequency might be chosen as $n\Omega_1$, i.e. some integer multiple of the fundamental solution frequency Ω_1. This can be arranged by setting to zero, the first $n-1$ Fourier coefficients in the excitation i.e. $C_0 = C_1 =, \ldots, C_{n-1} = 0$. Attention here however is focused on computing period-1 solutions (at the fundamental excitation frequency Ω_1) in response to multi-harmonic excitation with fundamental frequency Ω_1. It will therefore be assumed that the excitation coefficient C_1 is nonzero, and that the choice of the other excitation coefficients guarantees a periodic solution exists with fundamental excitation frequency Ω_1.

Suppose a trial solution y_t of Eq. (1) is considered, the equation error associated with Eq. (1) is then:

$$e(t) = \ddot{y}_t + F(y_t,\dot{y}_t) - f(t). \tag{3}$$

Now by defining two (Mickens) functions [24,26] as follows:

$$s_1(y_t) = (\ddot{y}_t + \Omega_1^2 y_t) \tag{4}$$

and

$$s_2(y_t) = \Omega_1^2 y_t - F(y_t,\dot{y}_t) + f(t) \tag{5}$$

and assuming $y(t)$ is a periodic solution of Eq. (1), then the function $s_2(y)$ has the effect of filtering-out the fundamental component in $y(t)$. The equation error (3) can be written in terms of these (Mickens) functions as follows:

$$e(t) = (\ddot{y}_t + \Omega_1^2 y_t) - (\Omega_1^2 y_t - F(y_t,\dot{y}_t) + f(t)) \tag{6}$$

or

$$e(y_t(t)) = s_1(y_t) - s_2(y_t). \tag{7}$$

Now if $y_t \to y(t)$, namely the trial solution converges in some sense to the true solution of Eq. (1), then from Eq. (7) the following condition must also hold:

$$\lim_{y_t \to y} s_1(y_t) = s_2(y_t). \tag{8}$$

For any periodic solution, the function $s_1(y_t)$, as defined by Eq. (4), has zero fundamental component. Therefore for any exact solution of Eq. (1), the function $s_2(y)$ will also have zero fundamental component. For arbitrary trial function values, the auxiliary functions $s_1(y_t)$ and $s_2(y_t)$ are in general very different—a property that will be exploited to good effect in a new iterative scheme explained shortly. Writing an assumed periodic solution of Eq. (1) as

$$y_t = y_{LF}(t) + y_{HF}(t) \tag{9}$$

namely in two separate parts: the first part made up of 'low frequency' (LF) components:

$$y_{LF}(t) = \frac{A_0}{2} + \sum_{m=1}^{k} A_m \cos(\Omega_m t + \Phi_m) \tag{10}$$

and the second part containing 'high frequency' (HF) components:

$$y_{HF}(t) = \sum_{m=k+1}^{\infty} A_m \cos(\Omega_m t + \Phi_m), \tag{11}$$

where $y_{HF}(t)$ usually has diminishingly small amplitudes. The "low" frequency components are defined as the part of the truncated Fourier series containing the k lowest frequency harmonics, whereas the "high" frequency components are the remaining components. In the proposed iterative scheme, the total number of

terms in the truncated version of Eq. (11) remains fixed. But the size of the two sets will vary since some of the components start-off in the "high" frequency group, but later become members of the "low" frequency group. The "low" frequency group will always start with just the mean (zero frequency), and the fundamental component. It will shortly be seen that the amplitudes and phases for the "low" frequency group are obtained by solving a system of FFT-generated algebraic equations, whereas the "high" frequency components are updated by iteration. The starting version of $y_{LF}(t)$ is a constant (not necessarily zero) plus a single harmonic function (representing the first harmonic in a Fourier series) i.e.

$$y_{LF}(t) = \frac{A_0}{2} + A_1 \cos(\Omega_1 t + \Phi_1). \tag{12}$$

Use of Eq. (9) in Eqs. (4) and (5) allows a re-arranged version of Eq. (7) to be written as

$$\begin{aligned} \ddot{y}_{LF} + \ddot{y}_{HF} + \Omega_1^2(y_{LF} + y_{HF}) &= \Omega_1^2(y_{LF} + y_{HF}) \\ &- F(y_{LF} + y_{HF}, \dot{y}_{LF} + \dot{y}_{HF}) + f(t) + e(y_{LF} + y_{HF}). \end{aligned} \tag{13}$$

On account of the version of $y_{LF}(t)$ in Eq. (12) having only a single harmonic at frequency Ω_1, Eq. (13) reduces to

$$\ddot{y}_{HF} + \Omega_1^2 y_{HF} = -\frac{A_0\Omega_1^2}{2} + \Omega_1^2(y_{LF} + y_{HF}) - F(y_{LF} + y_{HF}, \dot{y}_{LF} + \dot{y}_{HF}) + f(t) + e(y_{LF} + y_{HF}). \tag{14}$$

Now since both sides of Eq. (14) contain all harmonics except the fundamental, the right-hand-side of Eq. (14) can be represented by a Fourier series with all but fundamental frequency components, namely:

$$\begin{aligned} &-\frac{A_0\Omega_1^2}{2} + \Omega_1^2(y_{LF} + y_{HF}) - F(y_{LF} + y_{HF}, \dot{y}_{LF} + \dot{y}_{HF}) \\ &+ f(t) + e(y_{LF} + y_{HF}) = \frac{a_0}{2} + \sum_{n=2}^{\infty} a_n \cos(\Omega_n t) + b_n \sin(\Omega_n t). \end{aligned} \tag{15}$$

The forced (particular integral) solution of Eq. (14) can therefore be obtained explicitly as

$$y_{HFu} = \frac{a_0}{2\Omega_1^2} - \frac{1}{\Omega_1^2}\sum_{n=2}^{\infty} \frac{1}{(n^2-1)} a_n \cos(\Omega_n t) + b_n \sin(\Omega_n t), \tag{16}$$

where suffix u in y_{HFu} refers to an 'update'. The total solution of Eq. (14) (complementary function plus particular integral) is then

$$\begin{aligned} y_{HFu} &= \alpha \cos(\Omega_1 t) + \beta \sin(\Omega_1 t) \\ &+ \frac{1}{\Omega_1^2}\left\{\frac{a_0}{2} - \sum_{n=2}^{\infty} \frac{1}{(n^2-1)}\{a_n \cos(\Omega_n t) + b_n \sin(\Omega_n t)\}\right\}, \end{aligned} \tag{17}$$

where α and β are (unknown) constants of integration. The total updated form of Eq. (9) using Eq. (12), i.e. a single harmonic version of $y_{LF}(t)$, can further be written as

$$\begin{aligned} y_t(t) = &\frac{A_0}{2} + A_1 \cos(\Omega_1 t + \Phi_1) + \alpha \cos(\Omega_1 t) + \beta \sin(\Omega_1 t) \\ &+ \frac{1}{\Omega_1^2}\left\{\frac{a_0}{2} - \sum_{n=2}^{\infty} \frac{1}{(n^2-1)}\{a_n \cos(\Omega_n t) + b_n \sin(\Omega_n t)\}\right\} \end{aligned} \tag{18}$$

and without loss of generality, the constant terms and the complementary function (with unknown constants of integration α and β) in Eq. (18) can be combined to give

$$y_t(t) = \frac{A_0'}{2} + A_1' \cos(\Omega_1 t + \Phi_1') - \frac{1}{\Omega_1^2}\left\{\sum_{n=2}^{\infty} \frac{1}{(n^2-1)}\{a_n \cos(\Omega_n t) + b_n \sin(\Omega_n t)\}\right\}. \tag{19}$$

Now if the coefficients A_0, A_1, and Φ_1, in Eq. (12), and the function $y_{HF}(t)$ in Eq. (9) were chosen so that y_t were an exact solution, then $e(y_t(t)) = 0$ in Eq. (7), and the limit in Eq. (8) would be reached. Eq. (19) would

then correspond precisely to the same exact solution (where the undetermined coefficients must satisfy the condition $A'_0 = A_0$, $A'_1 = A_1$, and $\Phi'_1 = \Phi_1$). When the form of Eq. (9) is only an approximate solution of Eq. (1) but the correct nonzero equation-error term $e(y_t(t))$ is used in Eq. (15), then again the update y_{HFu} obtained from Eq. (16), would correspond to the original used. But when an approximate solution is used in Eq. (9), in which the equation-error term in Eq. (15) is set to zero, namely $e(y_t(t)) = 0$, then y_{HFu} obtained from Eq. (16) would in general be different from the original chosen since the limit in Eq. (8) would then be forced to hold. This updated version y_{HFu} would hopefully represent an improvement on the original. In fact repeated updating can start by first using a temporarily fixed (approximate) form of y_{HFu} and using for example, the HBM to find coefficients A_0, A_1, and Φ_1 in $y_{LF}(t) = (A_0/2) + A_1 \cos(\Omega_1 t + \Phi_1)$ as part of the complete trial solution $y_t = y_{LF}(t) + y_{HF}(t)$ in Eq. (1). Subsequent use of the updated higher frequency part y_{HFu} in Eq. (19), does however require coefficients A'_0, A'_1, and Φ'_1 to be updated (involving repeated application of the HBM). Continued use of this iterative process could give a better approximation after each iteration. But since Eq. (8) does not hold, except under exact conditions, there is no guarantee that the error would continue to reduce with each iteration. Continued reduction of the error is however made possible with the addition of more terms in Eq. (10). Generalising $y_{LF}(t)$ in Eq. (10) to include more terms in the low-frequency part of the solution namely

$$y_{LF}(t) = \frac{A_0}{2} + A_1 \cos(\Omega_1 t + \Phi_1) + A_2 \cos(\Omega_2 t + \Phi_2) + \cdots + A_k \cos(\Omega_k t + \Phi_k) \tag{20}$$

and initially assuming an approximate high frequency part $y_{HF}(t)$ in Eq. (9), leads to a more general form of Eq. (16). Namely by using an appropriate Fourier expansion of Eq. (15) and solving Eq. (13) for the non-constant part of the particular integral to give

$$y_{HFu} = -\frac{1}{\Omega_1^2}\left\{\sum_{n=2}^{\infty} \frac{1}{(n^2-1)}\{a_n \cos(\Omega_n t) + b_n \sin(\Omega_n t)\}\right\} - \left\{\sum_{K=2}^{k} A_K \cos(\Omega_K t + \Phi_K)\right\}. \tag{21}$$

But on account of the lower summation in Eq. (11) defining y_{HF}, low frequency terms up to the kth harmonic arising in both parts of Eq. (21) must cancel, reducing y_{HFu} to

$$y_{HFu} = -\frac{1}{\Omega_1^2}\left\{\sum_{n=k+1}^{\infty} \frac{1}{(n^2-1)}\{a_n \cos(\Omega_n t) + b_n \sin(\Omega_n t)\}\right\}. \tag{22}$$

The full form of the forced solution also involves the addition to Eq. (22) of the mean term $a_0/2\Omega_1^2$ which can be combined with the mean term in Eq. (20) to give the corresponding version of Eq. (19) as

$$y_t(t) = \frac{A'_0}{2} + A'_1 \cos(\Omega_1 t + \Phi'_1) + A_2 \cos(\Omega_2 t + \Phi_2) + \cdots + A_k \cos(\Omega_k t + \Phi_k) + y_{HFu}. \tag{23}$$

Now if the starting approximation y_{HF} is kept fixed, coefficients A_0, $A_1,\ldots,A_k$, and $\Phi_1,\Phi_2,\ldots,\Phi_k$ in Eq. (20) are first determined using the HBM to find the best trial solution $y_t = y_{LF}(t) + y_{HF}(t)$. Eq. (22) is then used to update the high frequency part $y_{HFu}(t)$, which is then used in the next iteration to obtain coefficients $A'_0, A'_1, A_2, \ldots, A_k, \ldots$ and $\Phi'_1, \Phi_2, \ldots, \Phi_k$ in Eq. (23) again using the HBM. This iteration process can be repeated to obtain a better approximation after each iteration. But again, although there is no guarantee that the equation error will continue to reduce, as more terms are used in Eq. (20), a corresponding reduction in the minimum error will result. This is the basis of the iterative scheme.

2.1. The computational details of the iterative scheme

Eq. (14), with Fourier series solution (16), forms the basis of the iteration scheme by starting-off assuming a single harmonic function represents a good approximation to the true solution. This in general makes use of the FFT to do three things: (i) to obtain exact time derivatives (in the frequency domain) for terms in both the equation error (3) and the right-hand-side of Eq. (14); (ii) to construct either algebraic equations or an objective function (for minimisation) using appropriate harmonic components of the equation error, (initially

involving just the mean and fundamental but later extended to k harmonic components); and (iii) to generate the Fourier coefficients of $s_2(y)$ as defined by Eq. (5) in particular the left-hand-side of Eq. (15) which (excluding the mean value and the error term) is needed for Fourier series solution (16) and later (22). The algorithm proceeds as follows:

Step 1: Start iteration at $i = 0$. Set $y_{HFi}(t) = 0$, i.e. assume $y_i = y_{LF} = (A_{0i}/2) + A_{1i}\cos(\Omega_1 t + \Phi_{1i})$.

Step 2: Solve for A_{0i}, A_{1i}, and Φ_{1i} via a one-term HBM solution of Eq. (1). In general this step is efficiently achieved using an FFT of the equation error $e(t_m)$ at N discrete time intervals of duration T/N over period T, in the form:

$$E(K) = \sum_{m=1}^{N} e(t_m)\mathrm{e}^{-\mathrm{j}2\pi K(m-1)/N}, \quad 0 \leqslant K \leqslant N-1. \tag{24}$$

The mean, and the real and imaginary parts of the complex fundamental component of $E(K)$ are then set to zero namely:

$$\{E(0)\} = \sum_{m=1}^{N} e(t_m) = g_0(A_{0i}, A_{1i}, \Phi_{1i}) = 0, \tag{25}$$

$$\mathrm{re}\{E(1)\} = \mathrm{re}\left\{\sum_{m=1}^{N} e(t_m)\mathrm{e}^{-\mathrm{j}2\pi(m-1)/N}\right\} = g_{1r}(A_{0i}, A_{1i}, \Phi_{1i}) = 0, \tag{26}$$

$$\mathrm{im}\{E(1)\} = \mathrm{im}\left\{\sum_{m=1}^{N} e(t_m)\mathrm{e}^{-\mathrm{j}2\pi(m-1)/N}\right\} = g_{1\mathrm{im}}(A_{0i}, A_{1i}, \Phi_{1i}) = 0, \tag{27}$$

leading to three algebraic equations for A_{0i}, A_{1i}, and Φ_{0i}. Alternatively, the sum of the squared absolute magnitudes of the equation error mean and fundamental component should have a well-behaved minimum at zero, allowing A_{0i}, A_{1i}, and Φ_{0i} to be obtained from an unconstrained least-square sum of objective function $g_1(A_{0i}, A_{1i}, \Phi_{1i})$ defined as

$$|E(0)|^2 + |E(1)|^2 = \sum_{K=0}^{1}\left|\sum_{m=1}^{N} e(t_m)\mathrm{e}^{-\mathrm{j}2\pi K(m-1)/N}\right|^2 = g_1(A_{0i}, A_{1i}, \Phi_{1i}). \tag{28}$$

Step 3: Obtain the Fourier components of Eq. (15) (omitting the equation error term). Then with coefficients a_n and b_n, obtain a first update estimate of $y_{HFi}(t)$, namely:

$$y_{HFi} = -\frac{1}{\Omega_1^2}\left\{\sum_{n=2}^{N/2}\frac{1}{(n^2-1)}a_n\cos(\Omega_n t) + b_n\sin(\Omega_n t)\right\}, \tag{29}$$

where suffix u has for convenience been omitted.

Step 4: Now generate an improved solution $y_{i+1} = (A_{0i+1}/2) + A_{1i+1}\cos(\Omega_1 t + \Phi_{1i+1}) + y_{HFi}(t)$, by solving for a new mean A_{0i+1}, and fundamental harmonic amplitude A_{1i+1} and phase Φ_{1i+1} using the HBM, and then by incrementing i and repeating steps 2–4, continue iterating a fixed number of times or until the rms value of the equation error (3) reaches a minimum.

Step 5: Next, use the final rms error values A_{0i}, A_{1i}, and Φ_{1i}, and the 2nd harmonic amplitude and phase associated with y_{HFi}, as the starting values for $A_{0i}, A_{1i}, \Phi_{1i}, A_{2i}$, and Φ_{2i} in a two-harmonic version of $y_{LF}(t)$ defined by Eq. (20) where the high frequency term $y_{HF}(t)$ is obtained from y_{HFi} by removing the lowest frequency component (i.e. the 2nd harmonic), namely:

$$y_t(t) = \frac{A_{0i}}{2} + A_{1i}\cos(\Omega_1 t + \Phi_{1i}) + A_{2i}\cos(\Omega_2 t + \Phi_{2i}) + y_{HF}(t). \tag{30}$$

In practice, a new HBM equation (to be minimised) can be constructed by keeping the y_{HF} part fixed, and by constructing the FFT of the equation error and then forming the sum of the first three squared

equation-error harmonics, namely:

$$|E(0)|^2 + |E(1)|^2 + |E(2)|^2 = \sum_{K=0}^{2} \left| \sum_{m=1}^{N} e(t_m) \mathrm{e}^{-\mathrm{j}2\pi K(m-1)/N} \right|^2 = g_2(A_{0i}, A_{1i}, \Phi_{1i}, A_{2i}, \Phi_{2i}). \tag{31}$$

Now with new y_{LFi} and y_{HFi}, obtain Fourier components for Eq. (15) (but again excluding the error term). The part of the solution to Eq. (14) to enable the high frequency update is then:

$$y_{HFi} = -\frac{1}{\Omega_1^2} \left\{ \sum_{n=3}^{N/2} \frac{1}{(n^2-1)} \{a_n \cos(\Omega_n t) + b_n \sin(\Omega_n t)\} \right\}. \tag{32}$$

Eq. (32) is then used in Eq. (30) to improve the harmonic balance solution. This is repeated, incrementing i a number of times or until the rms equation error reaches a new minimum.

Step 6: The lowest harmonic amplitude and phase in the final value of y_{HFi} are now used to augment the starting values in new additional terms for $y_{LF}(t)$ in Eq. (20), and where the remaining harmonics y_{HFi} are used as the new starting version of $y_{HF}(t)$. This will continue with an additional 3rd term, then a 4th term, and so on, adding more terms, in general giving rise to an approximate solution of the form:

$$y_t(t) = \frac{A_0}{2} + A_1 \cos(\Omega_1 t + \Phi_1) + A_2 \cos(\Omega_2 t + \Phi_2) + \cdots + A_k \cos(\Omega_k t + \Phi_k) + y_{HFi}(t). \tag{33}$$

Again the coefficients can be solved via the HBM as a least-square-error solution of

$$\sum_{K=0}^{k} |E(K)|^2 = \sum_{K=0}^{k} \left| \sum_{m=1}^{N} e(t_m) \mathrm{e}^{-\mathrm{j}2\pi K(m-1)/N} \right|^2 = g_k(A_0, A_1, \Phi_1, A_2, \Phi_2, \ldots, A_k, \Phi_k). \tag{34}$$

Step 7: The update in y_{HFi} generalises to

$$y_{HFi} = -\frac{1}{\Omega_1^2} \left\{ \sum_{n=k+1}^{N/2} \frac{1}{(n^2-1)} \{a_n \cos(\Omega_n t) + b_n \sin(\Omega_n t)\} \right\}. \tag{35}$$

This improvement process is continued until a value of k is reached using a particular version of Eq. (33), where the final rms equation-error is acceptably small.

2.2. The SF-HBM equations for the Duffing oscillator

As an example, the forms that Eqs. (1)–(15) take are of interest for the Duffing model:

$$\ddot{y} + 2\zeta\omega_n \dot{y} + \omega_n^2 y + \varepsilon y^3 = f(t). \tag{36}$$

The Duffing model belongs to the class of oscillators defined by Eq. (1) (with the exception that the excitation $f(t)$ is assumed to be multi-harmonic in the form given by Eq. (2) rather than just a single harmonic). When a trial solution y_t is assumed, the equation error associated with Eq. (36) is then:

$$e(t) = \ddot{y}_t + 2\zeta\omega_n \dot{y}_t + \omega_n^2 y_t + \varepsilon y_t^3 - f(t). \tag{37}$$

The definition of the $s_1(y)$ function Eq. (4) remains unchanged, but $s_2(y)$ specialises to

$$s_2(y_t) = (-2\zeta\omega_n \dot{y}_t - (\omega_n^2 - \Omega_1^2) y_t - \varepsilon y_t^3 + f(t)). \tag{38}$$

Assuming $y(t)$ is a periodic solution of Eq. (36), $s_2(y)$ has the effect of filtering-out the fundamental component in $y(t)$. The equation error (37) can also be written in the form:

$$e(t) = (\ddot{y}_t + \Omega_1^2 y_t) - (-2\zeta\omega_n \dot{y}_t - (\omega_n^2 - \Omega_1^2) y_t - \varepsilon y_t^3 + f(t)), \tag{39}$$

which on assuming a split solution of the form Eq. (9), allows Eq. (13) to be written:

$$\begin{aligned} \ddot{y}_{LF} + \ddot{y}_{HF} + \Omega_1^2 (y_{LF} + y_{HF}) = (&-2\zeta\omega_n (\dot{y}_{LF} + \dot{y}_{HF}) - (\omega_n^2 - \Omega_1^2)(y_{LF} + y_{HF}) \\ &- \varepsilon (y_{LF} + y_{HF})^3 + f(t)) + e(y_{LF} + y_{HF}), \end{aligned} \tag{40}$$

and for a single term low-frequency approximation Eq. (12) reduces to

$$\ddot{y}_{HF} + \Omega_1^2 y_{HF} = -\frac{A_0\Omega_1^2}{2} + (-2\zeta\omega_n(\dot{y}_{LF} + \dot{y}_{HF}) - (\omega_n^2 - \Omega_1^2)(y_{LF} + y_{HF}) - \varepsilon(y_{LF} + y_{HF})^3 + f(t)) + e(y_{LF} + y_{HF}) \tag{41}$$

and the form of Eq. (15) specialises to

$$-\frac{A_0\Omega_1^2}{2} + (-2\zeta\omega_n(\dot{y}_{LF} + \dot{y}_{HF}) - (\omega_n^2 - \Omega_1^2)(y_{LF} + y_{HF}) - \varepsilon(y_{LF} + y_{HF})^3 + f(t)) + e(y_{LF} + y_{HF}) = \frac{a_0}{2} + \sum_2^\infty a_n \cos(\Omega_n t) + b_n \sin(\Omega_n t), \tag{42}$$

where the Fourier components are needed for updating the high frequency part. The procedure then follows steps 1–7 as outlined in Section 2. To obtain the forced response at the driving frequency, the initial choice of starting frequency Ω_1, and the coefficients A_0, A_1, and Φ_1 in Eq. (12), play a significant role here but the convergence to a particular solution is not sensitively dependent. For a particular driving frequency these parameters can easily be selected to respectively give the high and low amplitude stable solutions. And a shift in phase of -90° from the high amplitude stable solution, gives for the Duffing oscillator, an unstable high amplitude solution. Although not the focus of this paper, it is not difficult to see how the choice of starting frequency Ω_1 can be used to target sub- and superharmonic resonances. The method will now be applied to particular cases of periodic responses at the driving frequency with multi-harmonic forcing.

3. Computation of period-1 oscillator responses using the SF-HBM

The SF-HBM proposed in Section 2 is now tested, first on a Duffing-type oscillator, and then for an oscillator with non-expansible nonlinear stiffness in the form of a 7th degree polynomial. The focus of attention here is on periodic solutions with the same period as the driving frequency. To assess the accuracy, capability, and efficiency of the method a comparison for the Duffing model is made with a conventional HBM. The conventional HBM makes heavy use of symbolic computation for generation of an appropriate system of nonlinear algebraic equations. First, details of this conventional method are given, followed by details of the test parameters, and then a comparison of the conventional method with the SF-HBM.

3.1. A conventional HBM—Algebraic equation generation via symbolic computation

Applications of the HBM, such as used in Refs. [4–12], generally follow a rather similar approach. There are some variants of the method, for example using prior knowledge to select a particular set of solution harmonics (as in Ref. [17] for reasons of efficiency), or for treatment of particular nonlinearities as in Ref. [14]. Here a 'conventional' HBM approach is described which is not generally restricted to use of these variants. This description includes the initial assumptions, preparation for use of symbolic computation, construction of the system of nonlinear algebraic equations for the Duffing oscillator, and then finally how these equations are solved. This conventional approach is used to benchmark the SF-HBM of Section 2 for generating periodic solutions at same fundamental period as the excitation. For application to the oscillator model (36), a zero-mean periodic excitation form of Eq. (2) is written explicitly in the form:

$$f(t) = \sum_{k=1}^{m} \alpha_k \cos(k\Omega_1 t) + \beta_k \sin(k\Omega_1 t). \tag{43}$$

The conventional HBM assumes a periodic system response directly in the form of a truncated Fourier series:

$$y(t) = A_{0c} + \sum_{n_c=1}^{r} A_{n_c} \cos(n_c\Omega_s t) + B_{n_c} \sin(n_c\Omega_s t), \tag{44}$$

where suffix c in n_c refers to 'conventional' HBM. To obtain periodic responses at the driving frequency, the fundamental response frequency $\Omega_s = \Omega_1$. The number of response frequencies r can be different from the number of excitation frequencies m. On substitution of Eq. (44) and its derivatives into the model (36), followed by algebraic manipulation and use of well-known trigonometric identities, an attempt can be made to equate (i.e. balance) particular harmonic terms on the left-hand side of the model to harmonic coefficients in the excitation—this creates a system of algebraic equations for the unknown coefficients in Eq. (44). The initial step requires a first-stage expansion of the cubic nonlinearity in Eq. (36) which in principle can be achieved via conventional manipulation (similar to Ref. [27]) in the form:

$$\begin{aligned}
&\sum_{n_c=1}^{r}(\omega_n^2-(n_c\Omega_1)^2+3\varepsilon A_{0c}^2)[A_{n_c}\cos(n_c\Omega_1 t)+B_{n_c}\sin(n_c\Omega_1 t)]\\
&\quad+\sum_{n_c=1}^{r}2n_c\xi\omega_n\Omega_1[-A_{n_c}\sin(n_c\Omega_1 t)+B_{n_c}\cos(n_c\Omega_1 t)]\\
&\quad+3A_{0c}\varepsilon\sum_{n_c=1}^{r}A_{n_c}^2\cos(n_c\Omega_1 t)^2+B_{n_c}^2\sin(n_c\Omega_1 t)^2\\
&\quad+\varepsilon\sum_{n_c=1}^{r}A_{n_c}^3\cos(n_c\Omega_1 t)^3+B_{n_c}^3\sin(n_c\Omega_1 t)^3\\
&\quad+3\varepsilon\left(\sum_{n_c=1}^{r}A_{n_c}^2\cos(n_c\Omega_1 t)^2B_{n_c}\sin(n_c\Omega_1 t)+A_{n_c}\cos(n_c\Omega_1 t)B_{n_c}^2\sin(n_c\Omega_1 t)^2\right)\\
&\quad+6A_{0c}\varepsilon\sum_{n_c=1}^{r}A_{n_c}\cos(n_c\Omega_1 t)B_{n_c}\sin(n_c\Omega_1 t)\\
&\quad+(\omega_n^2+\varepsilon A_{0c}^2)A_{0c}-\sum_{k=1}^{m}\alpha_k\cos(k\Omega_1 t)-\beta_k\sin(k\Omega_1 t)=0.
\end{aligned}\tag{45}$$

Expansion (45) shows products and higher power trigonometric terms—all of which require further expansion and simplification into individual trigonometric components before harmonic balance can occur. This simplification can be only achieved in practice for a relatively small number of terms in Eq. (44) i.e. 2 or 3 harmonics. When more terms are included, conventional algebraic manipulation rapidly becomes intractable which is one reason why more sophisticated expansions of the cubic term have been developed [14,20].

Alternatively a 'conventional' HBM approach can still be greatly extended by using symbolic processing tools to overcome the algebraic burden [15,16]. Here we describe an approach using the *maple* software to generate the equations—the details are summarised as follows: First the assumed trigonometric series for $f(t)$ and $y(t)$ in Eqs. (43) and (44), are created using the symbolic *sum* command. The first two symbolic derivatives are obtained by repeated application of the *diff* function to y. Symbolic y^3 is then constructed and the *expand* command is applied directly to it to generate the nonlinear terms in Eq. (45). Then after the symbolic representation of the system model Eq. (36) is constructed as a single function, the *simplify* command is applied directly to it to create a rather untidy Fourier series with many repeated terms in $\cos(k\Omega_1 t)$ and $\sin(k\Omega_1 t)$—this is by far the most computationally demanding step. Finally, using a loop (in conjunction with the *collect* command for $k \leqslant m$), the individual terms in the Fourier series are isolated into separate components. The algebraic equations are created in symbolic form by extracting the coefficient functions associated with each harmonic component. This is achieved by setting $k\Omega_1 t = 1$ and $k\Omega_1 t = \pi/2$ for all k (which avoids explicit use of Galerkin's method, thereby avoiding computationally demanding symbolic integration). An appropriate objective function can be created from the vector of symbolic algebraic equations for numerical computation using the *matlab* least square solver *lsqnonlin* (in a similar way as used in the SF-HBM of Section 2 to solve Eq. (34)). The main difference here is that the Jacobian matrix can also be generated directly in symbolic form and similarly converted for use in *lsqnonlin.* The Jacobian associated with Eq. (45) is however a full matrix and therefore does not enjoy, on large scale problems, the sort of sparsity structure often used to computational advantage in *lsqnonlin* (Jacobian construction can be an enormous task,

as in Ref. [21], where, written as a matrix equation, it runs to 7 pages in length). This 'conventional' HBM has been successfully used to generate and solve the algebraic equations associated with a large number of terms in Eq. (44). A practical limit arises on the number of terms, from the time needed to generate the system of HBM equations (particularly use of the Maple *simplify* command). On a PC (*Pentium 4*) for example, this limit occurs around 24 harmonics (49 unknowns) as explained now in a comparison with the SF-HBM.

3.2. A comparison of the SF-HBM and conventional HBM applied to the Duffing model

A test of the capability of the SF-HBM is now made for an oscillator model equation (36) with stiffness parameter values $\omega_n = 1.0$ and $\varepsilon = 0.75$, and with a moderately light damping level $\zeta = 0.05$. Four cases of zero-mean periodic excitation are considered starting with a single harmonic, and increasing to 24 harmonics (namely with 24 nonzero cosine and 24 sine terms in Eq. (43)).

Fig. 1 shows six cycles for each of the four forcing functions corresponding to 1, 6, 12, and 24 harmonics (the coefficients are given in Table 1 to an accuracy of four decimal places). The magnitude and frequency of the single harmonic forcing has been chosen to ensure that the oscillator response is significantly nonlinear. The harmonic coefficients for the 6, 12, and 24 cases were drawn randomly from a normal distribution $N(0,1)$ each with the same fundamental period as the single harmonic case. Fig. 2 shows a frequency response function for the oscillator with single harmonic forcing. Two specific points on the curve, namely a stable and one unstable solution at frequency ratio $\Omega/\omega_n = 2$, have been obtained using the conventional HBM up to its practical limit of 24 response harmonics (i.e. obtained by solving 49 nonlinear algebraic equations). The complete frequency response function was obtained over the entire frequency range using an Arc Length Continuation scheme, similar to that used in Ref. [17]. Stability of these points was confirmed using the nonlinear analysis method [17] adapted for use with the SF-HBM. The adaptation involves a two-stage

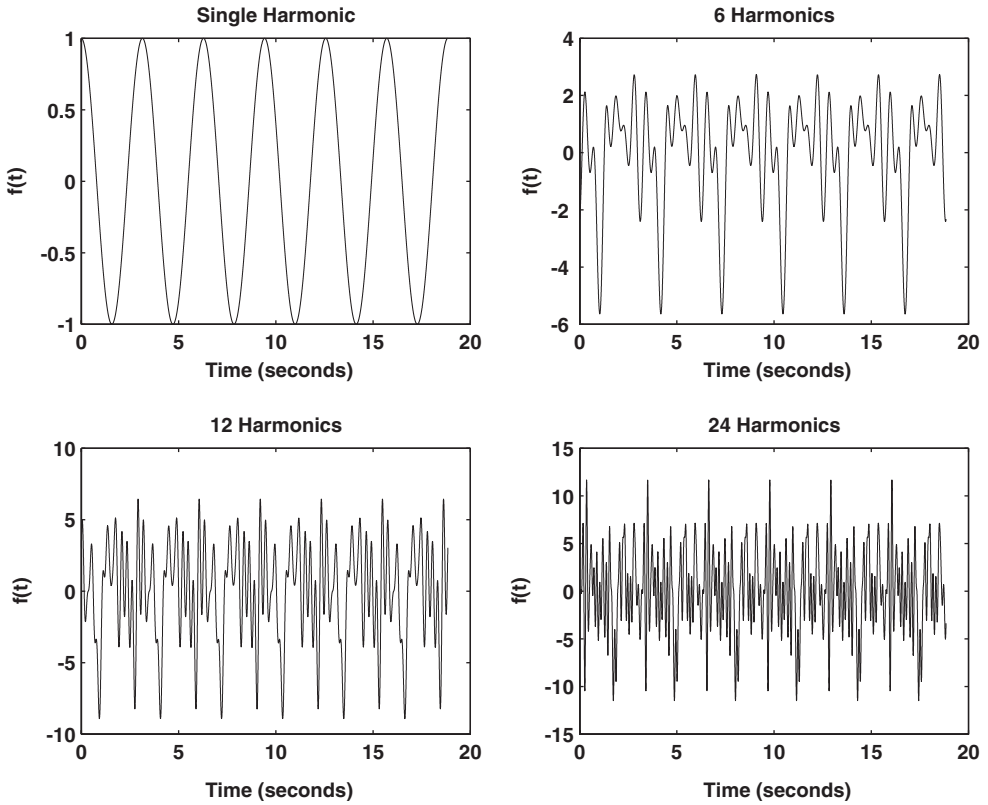

Fig. 1. Periodic excitation test cases showing six cycles for single, 6, 12, and 24 harmonics using the coefficient data in Table 1.

Table 1
Fourier coefficient magnitudes used in the test cases with multi-harmonic excitation

Forcing frequency ratio Ω/ω_n		Number of excitation harmonics (zero mean)							
		1		6		12		24	
		Cosine α_k	Sine β_k	Cosine α_k	Sine β_k	Cosine α_k	Sine β_k	Cosine α_k	Sine β_k
2	Magnitude of	1	0	0.1286	−1.3194	−0.5883	−0.6918	1.1908	0.0000
4	Fourier			0.6565	0.9312	2.1832	0.8580	−1.2025	−0.3179
6	coefficients			−1.1678	0.0112	−0.1364	1.2540	−0.0198	1.0950
8	= (shown to 4			−0.4606	−0.6451	0.1139	−1.5937	−0.1567	−1.8740
10	decimal places)			−0.2624	0.8057	1.0668	−1.4410	−1.6041	0.4282
12				−1.2132	0.2316	0.0593	0.5711	0.2573	0.8956
14						−0.0956	−0.3999	−1.0565	0.7310
16						−0.8323	0.6900	1.4151	0.5779
18						0.2944	0.8156	−0.8051	0.0403
20						−1.3362	0.7119	0.5287	0.6771
22						0.7143	1.2902	0.2193	0.5689
24						1.6236	0.6686	−0.9219	−0.2556
26								−2.1707	−0.3775
28								−0.0592	−0.2959
30								−1.0106	−1.4751
32								0.6145	−0.2340
34								0.5077	0.1184
36								1.6924	0.3148
38								0.5913	1.4435
40								−0.6436	−0.3510
42								0.3803	0.6232
44								−1.0091	0.7990
46								−0.0195	0.9409
48								−0.0482	−0.9921

transformation of the wholly real Jacobian (used in the SF-HBM) to the complex form in Ref. [17]. This transformation is singular if particular response harmonic amplitudes approach zero but the problem can be avoided by removing (from the Jacobian) rows and columns (associated with near-zero amplitudes).

Focusing initially on the stable HBM solution, Fig. 3a shows the rms equation error obtained using the conventional HBM as the number of harmonics in the solution is increased. To generate this information an increasingly large system of nonlinear algebraic equations up to a practical maximum number of 24 must be repeatedly generated and repeatedly solved. Fig. 3b shows the absolute magnitude of the harmonics obtained for the 24 harmonic solution. Fig. 4a shows the equation error rms for the same stable solution obtained using the SF-HBM over 2^6 discrete time points. This information does not correspond directly to that shown in Fig. 3a since here, the equation error rms is shown as a function of the total number of iterations (described in steps 1–6 in Section 2). The errors associated with each iteration are shown with a '●' symbol, where four iterations have been made following introduction of each additional low-frequency harmonic (the last iteration prior to the introduction of a new low-frequency harmonic is shown overlaid with '○' symbol) up to a maximum of 6 low-frequency harmonics. All of the equation error rms values shown in Fig. 4a correspond to the use of all 32 (low and high frequency) harmonics starting with the mean value plus a single cosine term with unknown amplitude and phase. Fig. 4b shows the absolute magnitude of all 32 harmonics obtained with the SF-HBM for the converged case of 6 low-frequency harmonics. This figure can be compared with Fig. 3b up to 24 harmonics (the limitation of the conventional HBM). Fig. 4c shows the converged (stable) solution obtained with the SF-HBM compared with the starting low-frequency harmonic, for which the mean is assumed to be zero and the amplitude and phase are starting guesses.

Corresponding results for the unstable solution of the oscillator with the same single harmonic excitation at frequency ratio $\Omega/\omega_n = 2$ (identified in Fig. 2), are shown in Figs. 5 and 6. Fig. 5a shows the equation error

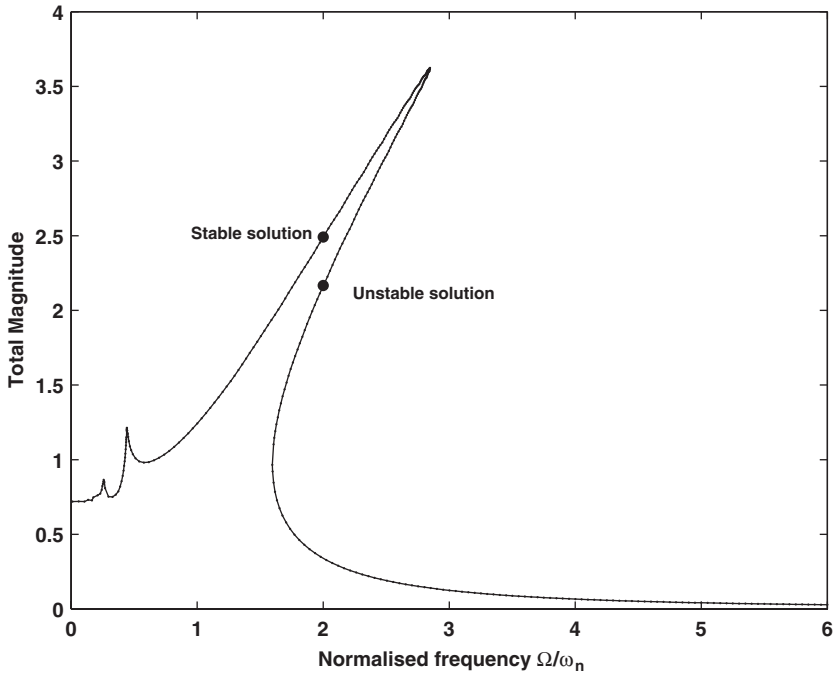

Fig. 2. Frequency response function for Duffing oscillator with single-harmonic forcing showing stable and unstable solution response amplitude at $\Omega/\omega_n = 2$ obtained via conventional HBM using 24 response harmonics.

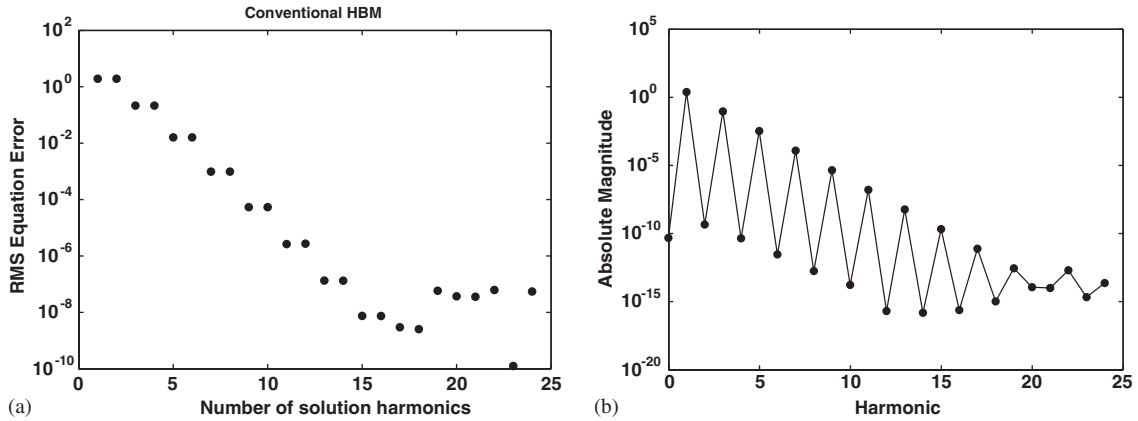

Fig. 3. Duffing oscillator stable solution information at $\Omega/\omega_n = 2$ computed via conventional HBM for single-harmonic forcing: (a) equation error rms as more harmonics used to generate solution and (b) absolute magnitudes when 24 response harmonics used.

rms values, again as more terms are assumed in the solution obtained via the conventional HBM. Fig. 5b shows the absolute magnitudes of the harmonics for the nominally converged case of 24 response harmonics. Fig. 6a shows the SF-HBM rms equation errors as a function of iteration number, where again 2^6 discrete time points have been used, and a maximum of 6 low-frequency harmonics. Fig. 6b shows the absolute magnitudes of the total 32 harmonics for 6 low-frequency harmonics. And in Fig. 6c, the converged response prediction with 6 low-frequency harmonics is compared with the starting low-frequency harmonic (again starting with a mean zero). The main difference between the stable and unstable starting cosine function is that the guessed phase for the unstable solution is delayed roughly by 90° compared with the stable solution.

Turning attention to the test results for an oscillator with the polyharmonic excitation involving 6, 12, and 24 harmonic periodic forcing shown in Fig. 1—the same model parameters are used as previously for single

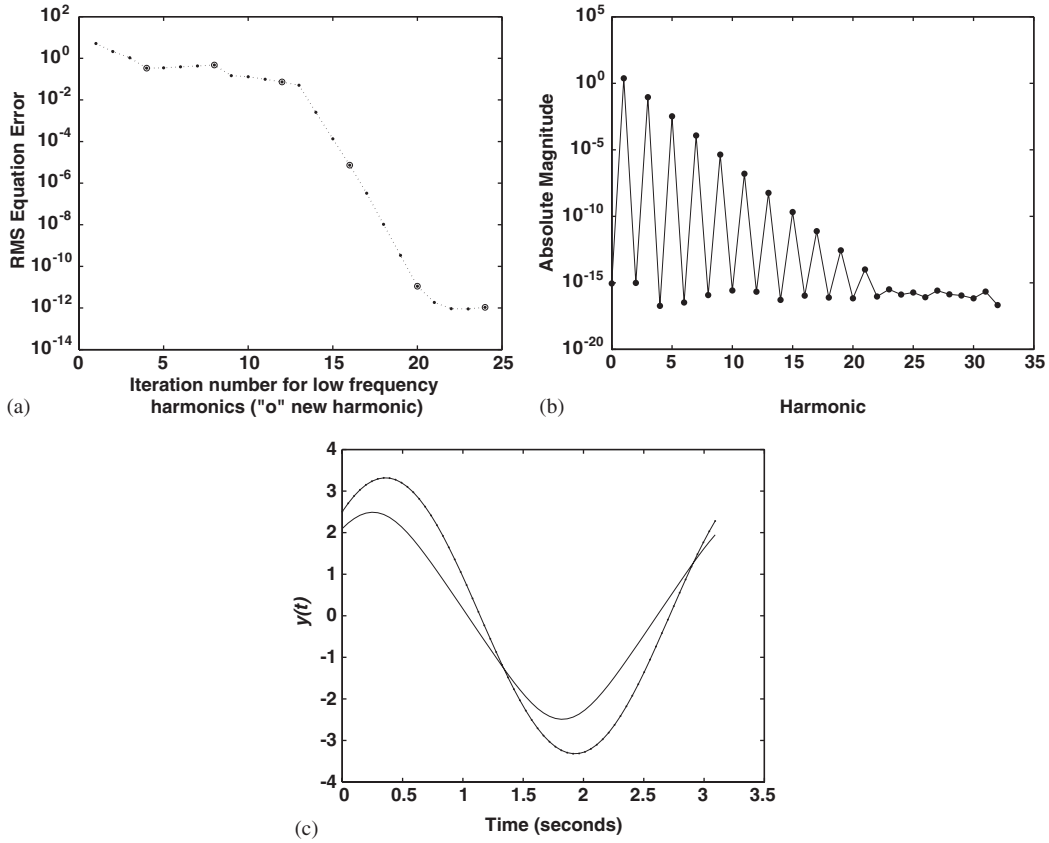

Fig. 4. Duffing oscillator stable solution information at $\Omega/\omega_n = 2$ computed via SF-HBM for single-harmonic forcing over 64 discrete time points: (a) equation error rms as a function of iteration number (shown as a ● symbol) with four iterations as each of the six low-frequency harmonics is introduced (4th iteration shown overlaid with ○ symbol); (b) absolute magnitudes of the total 32 response harmonics and (c) stable periodic solution compared with starting single harmonic.

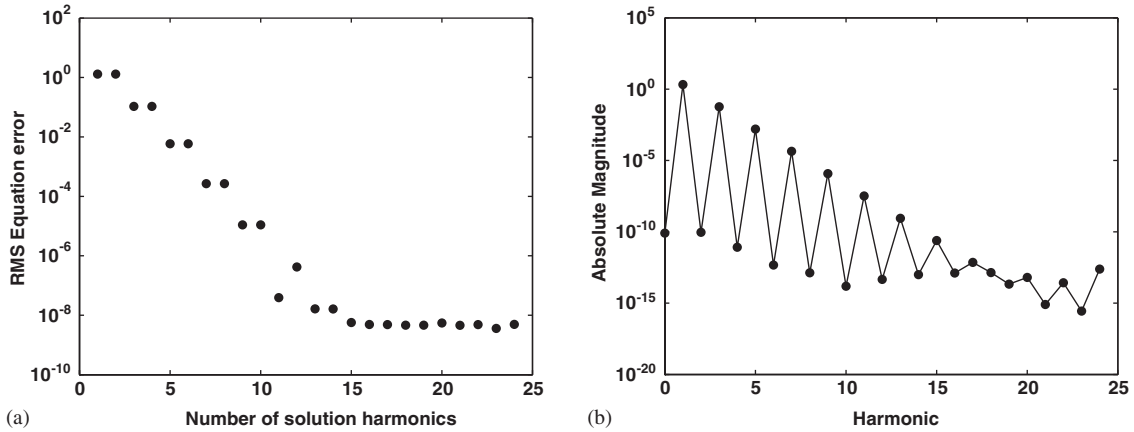

Fig. 5. Duffing oscillator unstable solution information at $\Omega/\omega_n = 2$ computed via conventional HBM for single-harmonic forcing: (a) equation error rms as more harmonics used to generate solution and (b) absolute magnitudes when 24 response harmonics used.

harmonic forcing. Fig. 7a shows for 6-harmonic forcing, the rms equation errors obtained with the conventional HBM as more harmonics are used to generate a stable solution up to the practical maximum of 24 harmonics. Fig. 7b shows for the 24-harmonic solution, the absolute magnitudes of the Fourier

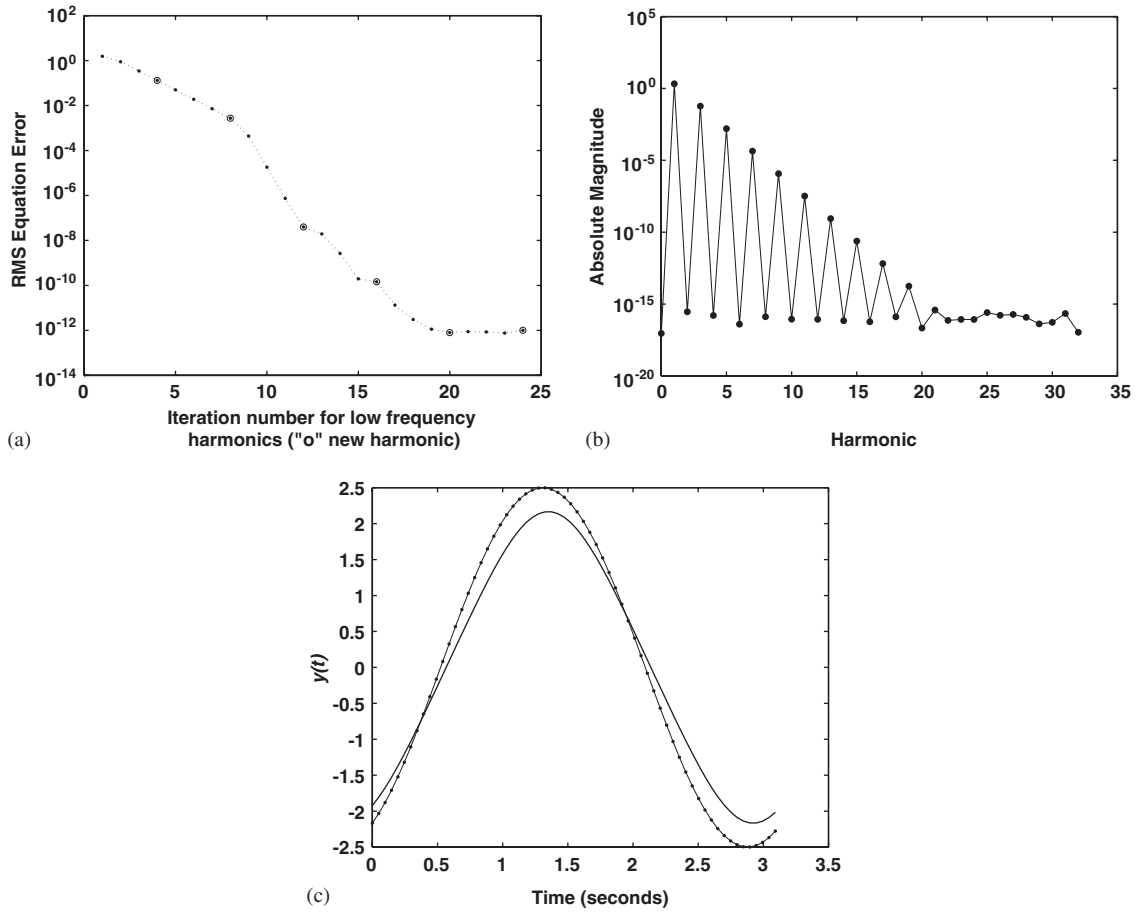

Fig. 6. Duffing oscillator unstable solution information at $\Omega/\omega_n = 2$ computed via SF-HBM for single-harmonic forcing over 64 discrete time points: (a) equation error rms as a function of iteration number (shown as a ● symbol) with four iterations as each of the six low-frequency harmonics is introduced (4th iteration shown overlaid with ○ symbol); (b) absolute magnitudes of the total 32 response harmonics and (c) stable periodic solution compared with starting single harmonic.

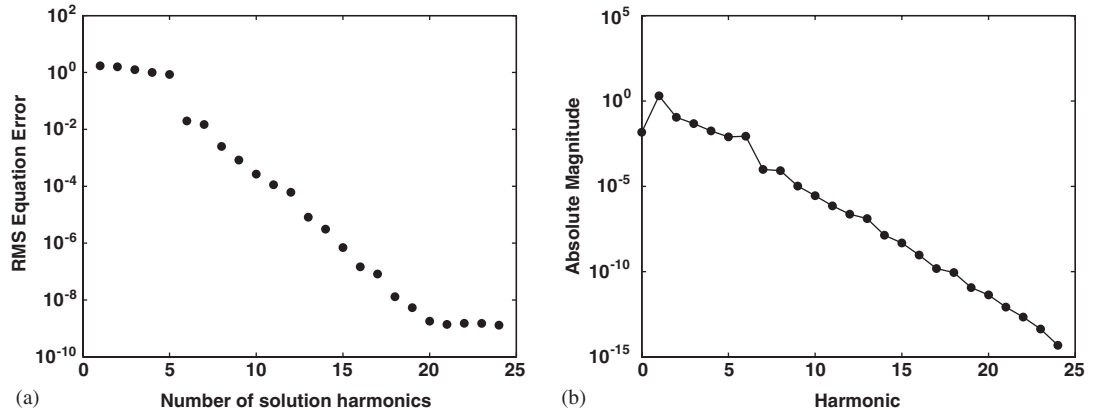

Fig. 7. Oscillator stable solution information at $\Omega/\omega_n = 2$ computed via conventional HBM for 6-harmonic forcing: (a) equation error rms as more harmonics used to generate solution and (b) absolute magnitudes when 24 response harmonics used.

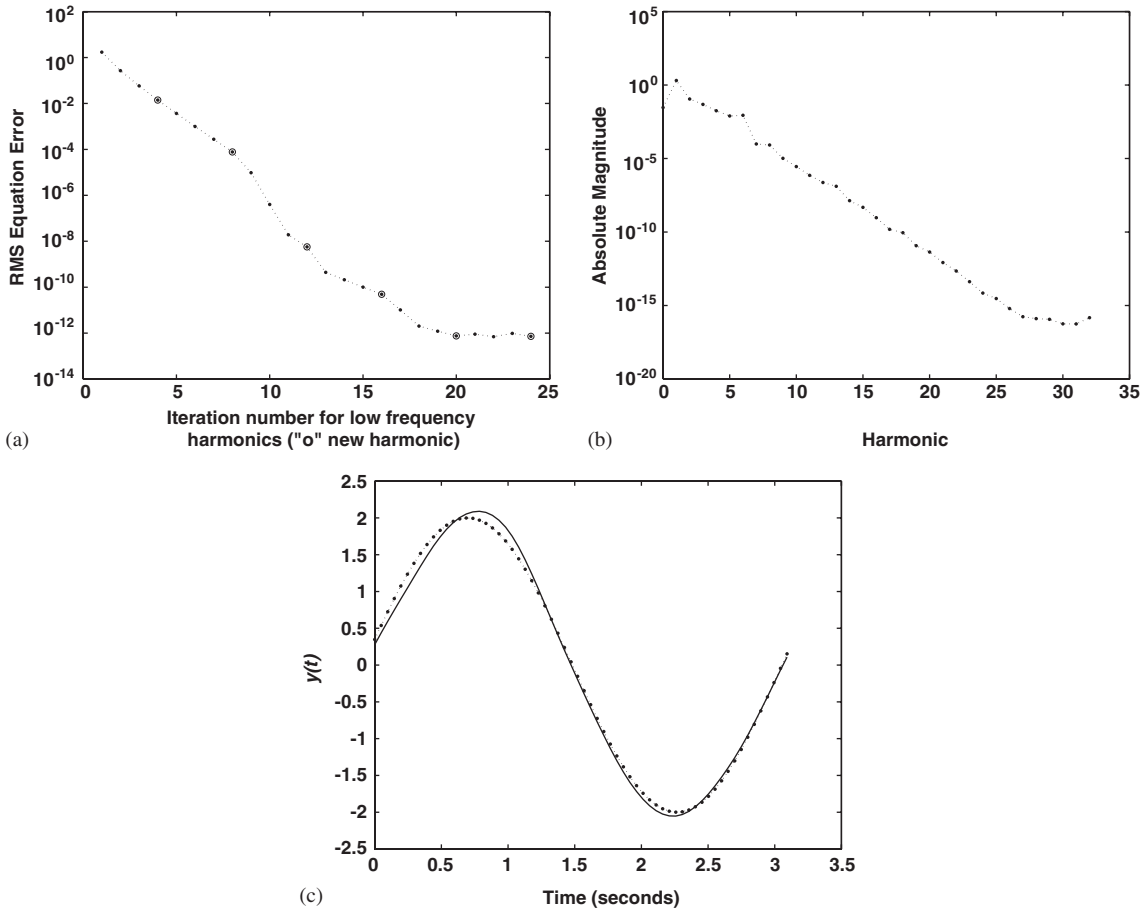

Fig. 8. Oscillator stable solution information at $\Omega/\omega_n = 2$ computed via SF-HBM for 6-harmonic forcing over 64 discrete time points: (a) equation error rms as a function of iteration number (shown as a ● symbol) with four iterations as each of the six low-frequency harmonics is introduced (4th iteration shown overlaid with ○ symbol); (b) absolute magnitudes of the total 32 response harmonics and (c) stable periodic solution compared with starting single harmonic.

Coefficients. Fig. 8b shows for the 6-harmonic forcing case the rms equation errors obtained with the SF-HBM again using four iterations per additional low-frequency harmonic (with convergence at 6 low-frequency harmonics) and again over 2^6 discrete time points. Fig. 8b shows the absolute magnitudes of the total 32 harmonics for the converged solution. Fig. 8c compares one cycle of the corresponding converged periodic solution with the starting low-frequency harmonic, again starting with an assumed zero mean.

Fig. 9a gives the 12-harmonic forcing rms equation errors obtained using the conventional HBM as a function of the number of harmonics used to generate the solution, and Fig. 9b gives the absolute magnitudes of the 24-harmonic solution. Fig. 10a shows corresponding rms equation errors using the SF-HBM with four iterations per additional low-frequency harmonic (up to a maximum of 6) over 2^8 discrete time points (the increase over the 1 and 6-harmonic case being needed for convergence). Fig. 10b shows the absolute magnitudes of the harmonic for the converged solution showing the total of 128 low and high frequency components. Fig. 10c shows a comparison of the converged solution with the starting low-frequency harmonic, again assuming zero mean.

For the 24-harmonic forcing case, Fig. 11a shows the rms equation errors as more harmonics are used to generate the solution in the conventional HBM. Fig. 11b shows the absolute magnitudes of the Fourier coefficients for the practical limitation of 24 response harmonics. Fig. 12a gives the corresponding equation errors using the SF-HBM, again with four iterations per additional low-frequency harmonic (up to a maximum of eight) over 2^8 discrete time points—the increase from 6 to 8 low-frequency harmonics being

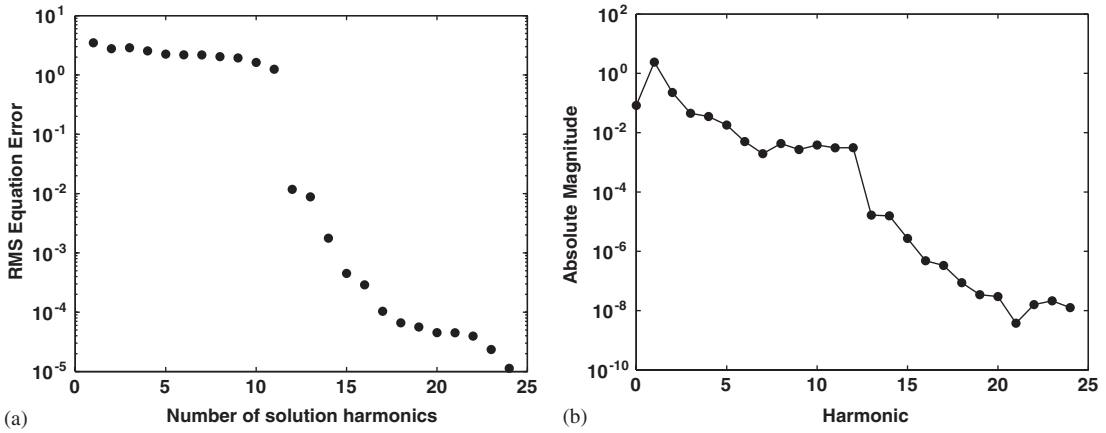

Fig. 9. Oscillator stable solution information at $\Omega/\omega_n = 2$ computed via conventional HBM for 12-harmonic forcing: (a) equation error rms as more harmonics used to generate solution and (b) absolute magnitudes when 24 response harmonics used.

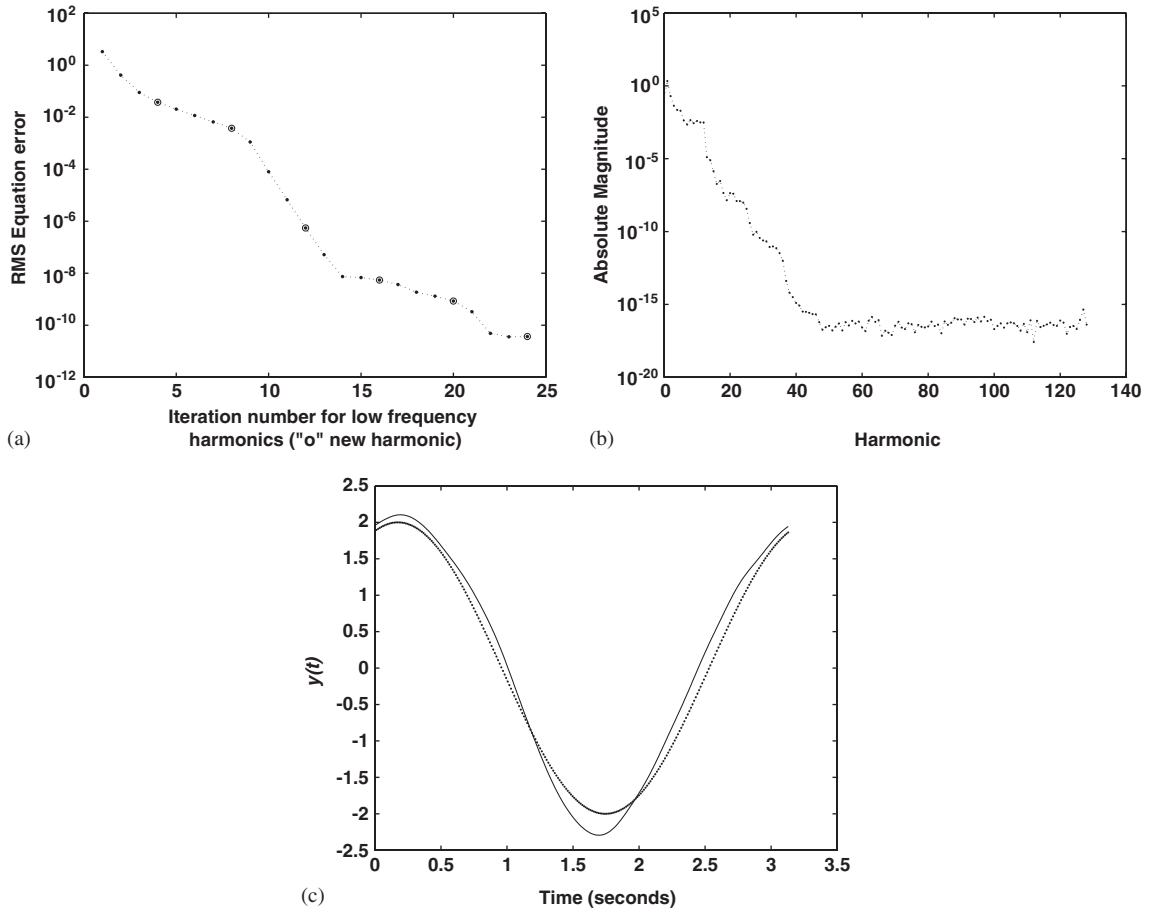

Fig. 10. Oscillator stable solution information at $\Omega/\omega_n = 2$ computed via SF-HBM for 12-harmonic forcing over 256 discrete time points: (a) equation error rms as a function of iteration number (shown as a ● symbol) with four iterations as each of the 6 low-frequency harmonics is introduced (4th iteration shown overlaid with ○ symbol); (b) absolute magnitudes of the total 128 response harmonics and (c) stable periodic solution compared with starting single harmonic.

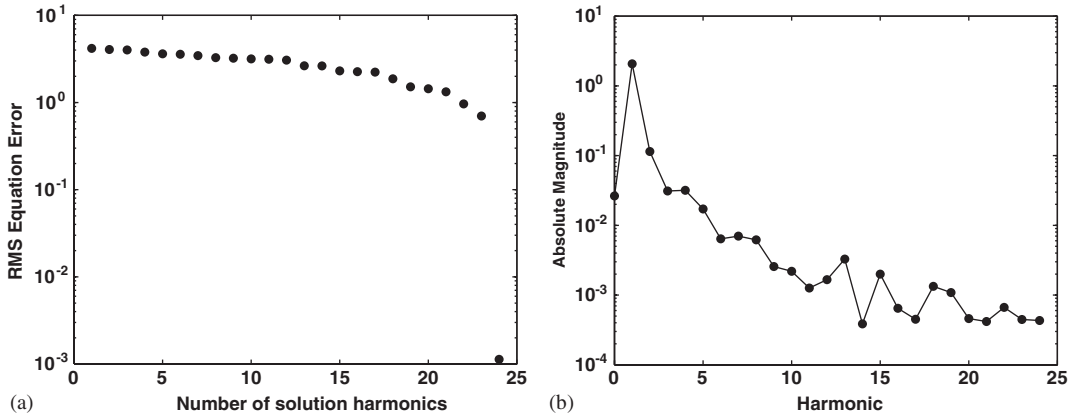

Fig. 11. Oscillator stable solution information at $\Omega/\omega_n = 2$ computed via conventional HBM for 24-harmonic forcing: (a) equation error rms as more harmonics used to generate solution and (b) absolute magnitudes when 24 response harmonics used.

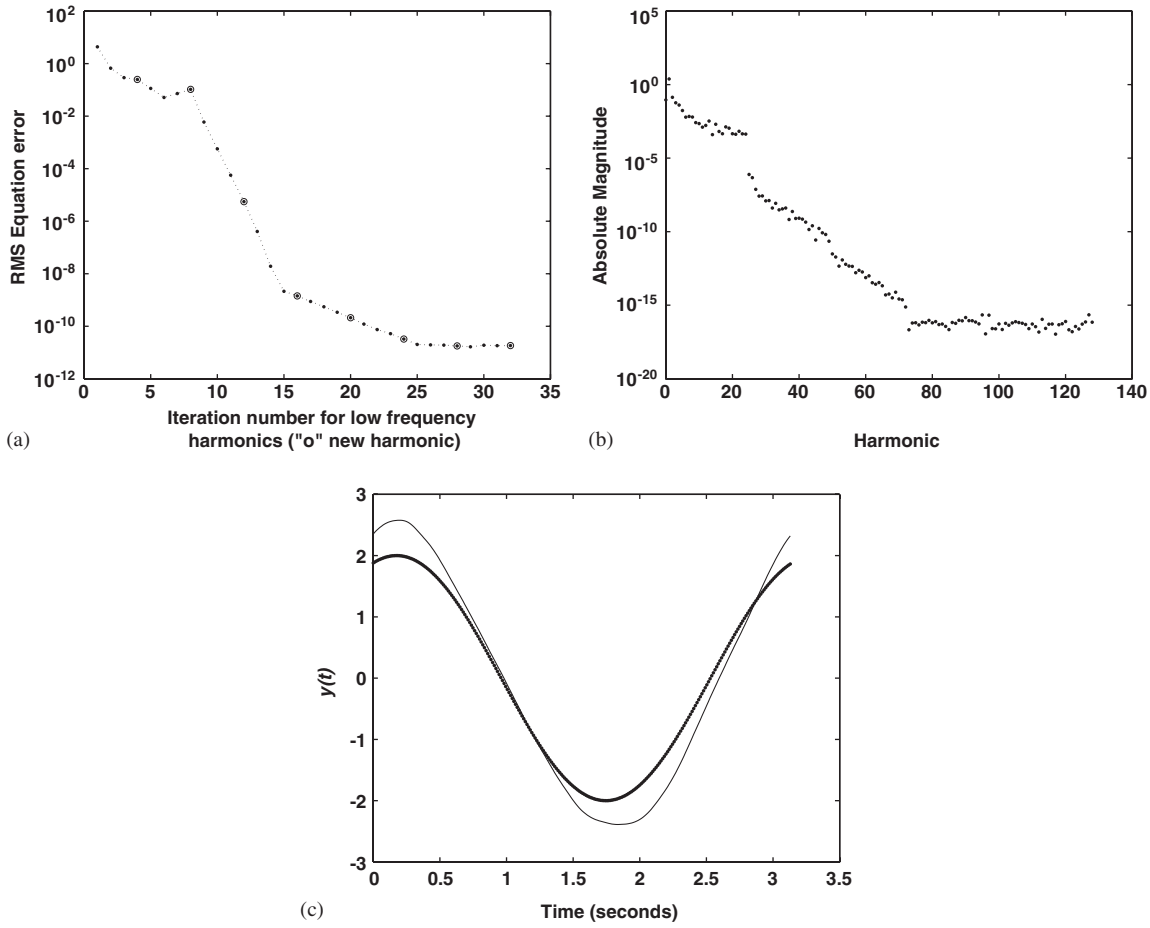

Fig. 12. Oscillator stable solution information at $\Omega/\omega_n = 2$ computed via SF-HBM for 24-harmonic forcing over 256 discrete time points: (a) equation error rms as a function of iteration number (shown as a ● symbol) with four iterations as each of the 8 low-frequency harmonics is introduced (4th iteration shown overlaid with ○ symbol); (b) absolute magnitudes of the total 128 response harmonics and (c) stable periodic solution compared with starting single harmonic.

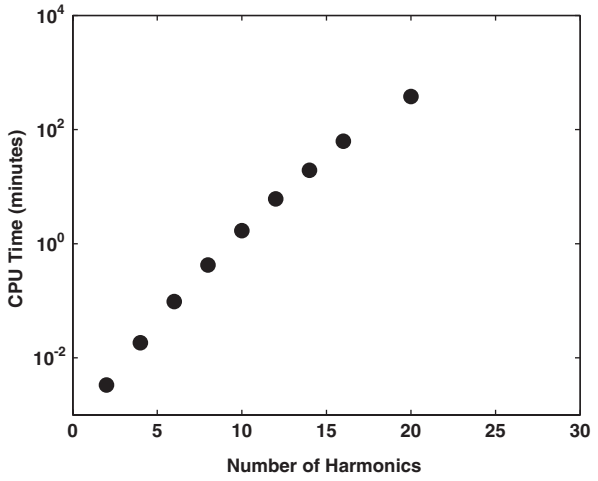

Fig. 13. Symbolic computation time (in minutes) as a function of the number of harmonics, needed to expand the cubic nonlinearity (on a Pentium 4 PC) for constructing the conventional HBM algebraic equations to obtain the solution of the Duffing oscillator.

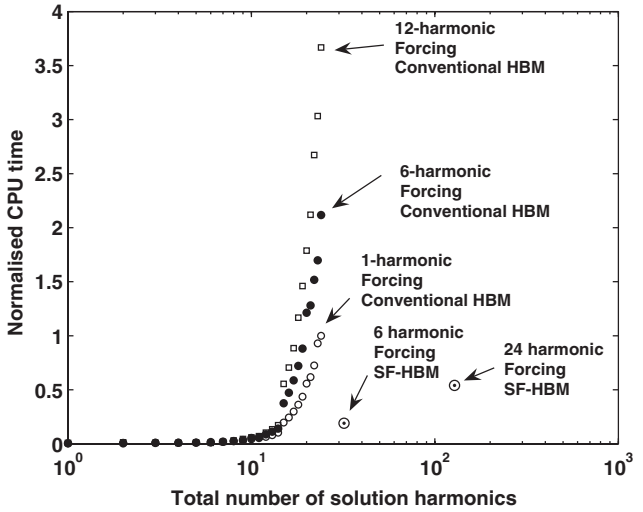

Fig. 14. Normalised computational time to obtain oscillator solution information at $\Omega/\omega_n = 2$ via conventional HBM compared with SF-HBM for 1-, 6-, 12- and 24-harmonic forcing.

needed for convergence. Fig. 12b shows the absolute Fourier coefficient magnitudes for the SF-HBM converged solution, and Fig. 12c compares one cycle of this solution with the guessed zero-mean starting low-frequency harmonic.

With regard to the computational efficiency of the SF-HBM, it is of interest to assess the relative computational efficiency of the method compared with the time needed for the conventional HBM to obtain a converged solution. In general using the conventional HBM, there are two main tasks that contribute to the computational burden: (i) the computing time needed to generate the system of HBM nonlinear algebraic equations (here via symbolic computation), and (ii) the time taken to obtain a converged numerical solution from the generated system of algebraic equations. Since the SF-HBM is implemented numerically, making full use of the FFT, each algebraic equation is generated numerically only when it is needed (in the form of Eq. (34)). Most of the computational burden therefore is taken-up in task (ii) and is not separate from the relatively insignificant contribution needed for equation generation. By contrast, Fig. 13 shows equation

generation times for the conventional method on a Pentium 4 using the *maple* symbolic software. Regarding the solution time needed to solve for the unknown harmonic coefficients task (ii) can be completely separated from (i). Fig. 14 shows for the conventional HBM, normalised CPU times needed to generate the solution for the 1-, 6- and 12-harmonic forcing, shown as a function of the number of harmonics used in the solution. Normalisation is based on the CPU time taken to obtain a converged 24-harmonic solution for the oscillator with single harmonic forcing. Also shown on Fig. 14, are the SF-HBM normalised CPU times needed to obtain converged solutions for the 6- and 24-harmonic forcing, noting that these SF-HBM CPU times are the total times needed for both tasks (i) and tasks (ii).

Finally, for the Duffing model, it should be mentioned for the conventional HBM, the least-square solver was compared using both a user-supplied closed-form Jacobian (generated symbolically), and an internally generated Jacobian based on finite differences (the SF-HBM always uses a numerically generated Jacobian). It was found that the accuracy of the conventional HBM was virtually identical whichever Jacobian was used. Also, there were only marginal improvements in efficiency using the closed form Jacobian where the speed advantage remained less than a factor 2.

3.2.1. *Discussion of results for the Duffing model*

First regarding the overall effect of introducing multi-harmonic forcing on the performance of the conventional HBM for response prediction at the fundamental driving frequency, Figs. 3a (for stable 1-harmonic forcing), Fig. 7a (for 6-harmonic forcing), Fig. 9a (for 12-harmonic forcing), and Fig. 11a (for 24-harmonic forcing) clearly show that as more forcing harmonics are introduced, correspondingly more harmonics are needed in the response to achieve a specified level of accuracy in the solution. The respective number of harmonics needed to achieve an equation error rms level of 2^{-6} starts at 24 coefficients for 1-harmonic forcing (i.e. 12 cosine + 12 sine coefficients), 31 coefficients for 6-harmonic forcing (i.e. the mean value + 15 cosine + 15 sine coefficients), and 49 + coefficients for 12-harmonic forcing (i.e. the mean value + 24 cosine + 24 sine coefficients). For 24-harmonic forcing it is clear in Fig. 11a, that the limitation of the conventional HBM is fully realised where the benchmark rms error level of 2^{-6} is far from reached. This is caused by not being able to construct a system greater than 49 algebraic equation. It is clear from Fig. 12b using the SF-HBM, that for 24-harmonic forcing around 140 algebraic equations would be needed (70 harmonics) to get complete convergence using a conventional HBM. Regarding the accuracy and convergence of the SF-HBM, Fig. 4a, Fig. 8a, and Fig. 10a clearly show that it is possible to obtain a highly accurate periodic response using as few as 6 low-frequency harmonics. Only a crude guess is needed for the starting low-frequency harmonic followed by only four iteration for each new additional low-frequency harmonic. Even when 24-harmonic forcing is introduced, the same level of accuracy is achieved with just eight low-frequency harmonics. The full bandwidth of the response however depends only on the number of discrete time points which, as Figs. 10b and 12b show, allow a very high bandwidth to be obtained. One point of interest to note regards the zero harmonic coefficient (response mean) value obtained (with both methods) as shown in Figs. 3b, 7b, and 9b (for the conventional HBM), and 4b, 8b, and 10b (for the SF-HBM). For single-harmonic forcing this is zero. But for multi-harmonic forcing the mean periodic response is not zero. This represents an initially unexpected loss of symmetry that can be explained by considering the equation error with just two-harmonic forcing terms assuming a response with zero mean. It is easy to show that the mean of the equation error cannot then be set to zero regardless of how many solution harmonics are used. A nonzero mean is needed to do this. This was not wholly expected and indeed the implications are quite profound.

As to the equation generation time and computational efficiency Fig. 13 shows that beyond 20 harmonics, equation generation using the conventional HBM becomes impractical in terms of time taken. Fig. 14 clearly shows that the SF-HBM allows an increase in bandwidth with only marginal growth in computational cost—this is in stark contrast to the conventional HBM cost which grows rapidly with the number of forcing harmonics and the number of response harmonics. Fig. 14 shows that even when the size of the system of algebraic equations remains fixed, the larger the number of forcing harmonics (and therefore more inhomogeneous algebraic equations) the greater the computational cost. This dependence is not significant for the SF-HBM and therefore opens-up new possibilities for generation of a ultra high-bandwidth nonlinear oscillator responses to a large number of forcing harmonics.

3.3. Period-1 response computation for an oscillator with non-expansible stiffness

The use of FFT generated algebraic equations allows a wide class of non-expansible nonlinearities to be handled. Even a 5th power nonlinearity for example is non-expansible in practice since it is quite intractable to construct algebraic relations between the coefficients of a Fourier series, and the coefficients in the related Fourier series (obtained by raising the original series to power 5). A test is now undertaken for an oscillator with a 7th power nonlinearity as follows:

$$\ddot{y} + 2\zeta\omega_n\dot{y} + \omega_n^2 y + \varepsilon y^7 = f(t). \tag{46}$$

The SF-HBM has been used to compute period-1 responses for both single and multi-harmonic forcing for the model (46) with the magnitudes of stiffness parameter values $\omega_n = 1.0$, and $\varepsilon = 0.2$, and with damping factor $\zeta = 0.04$. Three cases of periodic excitation are considered namely single-, 12-, and 24-harmonic forcing corresponding to the coefficients in Table 1. Fig. 15 shows the entire frequency response function computed using the SF-HBM for single-harmonic forcing.

Fig. 16a shows the equation error rms for the solution with 12-harmonic obtained using SF-HBM over 2^8 discrete time points. Again the equation error rms is shown as a function of the total number of iterations shown with a '●' symbol, where four iterations have been made for each additional low-frequency harmonic (the last iteration prior to the introduction of each new low-frequency harmonic is again shown overlaid with '○' symbol) up to a maximum of 10 low-frequency harmonics. All of the equation error rms values shown in Fig. 16a correspond to the use of all 128 (low and high frequency) harmonics starting with the mean value plus a single cosine term with unknown amplitude and phase. Fig. 16b shows the absolute magnitude of all 128 harmonics obtained with the SF-HBM for the converged case of 10 low-frequency harmonics. Fig. 16c shows the converged solution computed with the SF-HBM compared with the starting low-frequency harmonic, for which the mean is assumed to be zero and the amplitude and phase are starting guesses. Corresponding results for the computed period-1 solution with 24-harmonic forcing are shown in Fig. 17a (rms errors), Fig. 17b (absolute magnitudes), and Fig. 17c (solution compared with starting harmonic). Figs. 16a and 17a clearly demonstrate that the SF-HBM is very capable of computing an accurate period-1 responses for an oscillator with non-expansible nonlinearity.

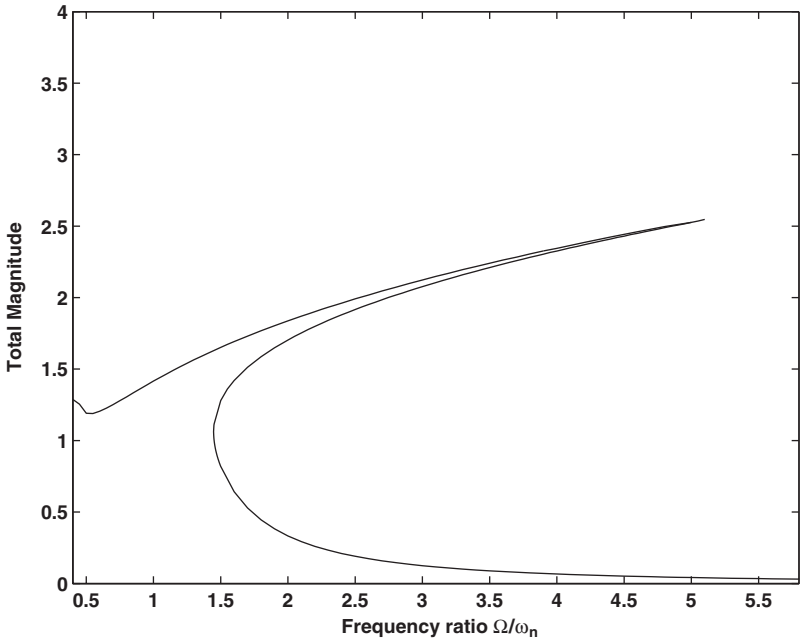

Fig. 15. Frequency response function computed via the SF-HBM for the oscillator with 7th degree stiffness and single-harmonic forcing.

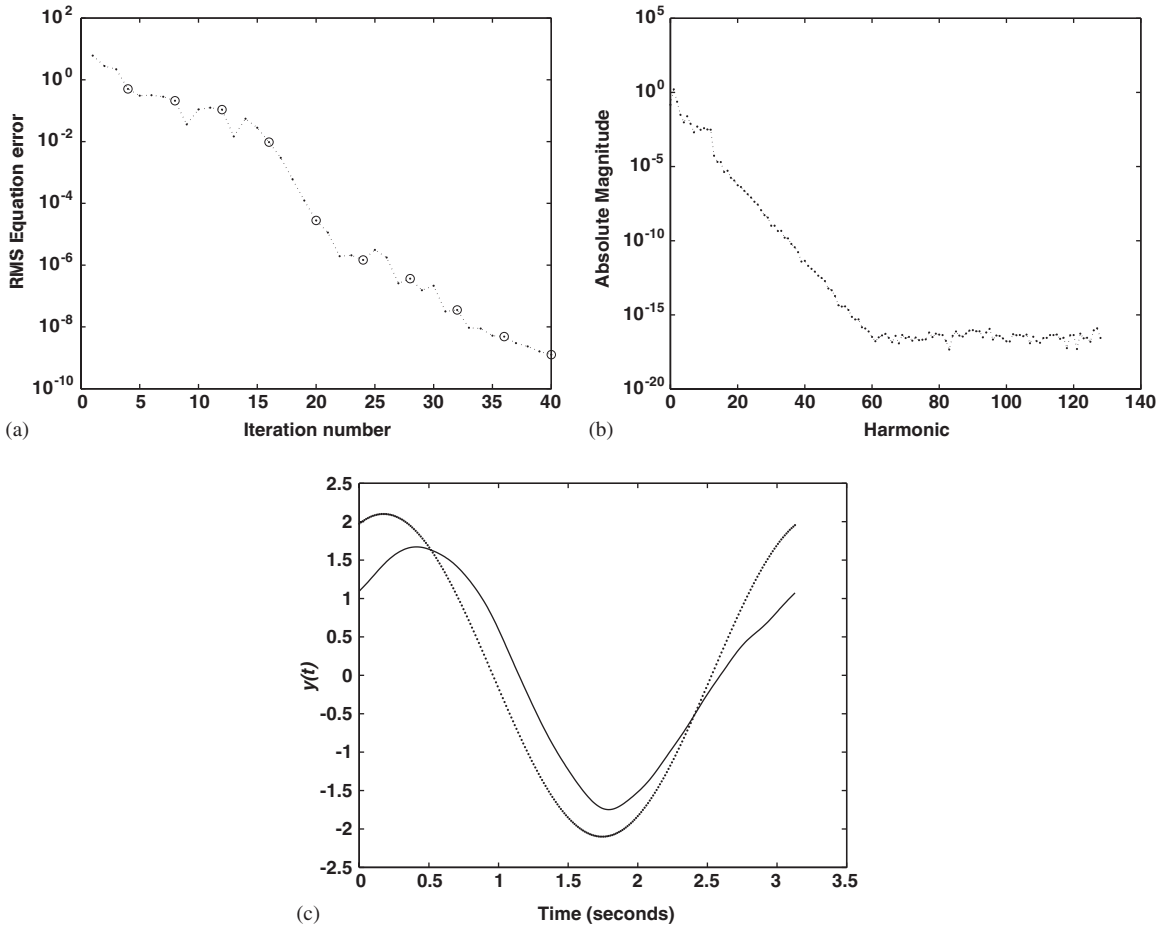

Fig. 16. Solution information at $\Omega/\omega_n = 2$ for oscillator with 7th degree stiffness computed via SF-HBM for 12-harmonic forcing over 256 discrete time points: (a) equation error rms as a function of iteration number (shown as a ● symbol) with four iterations as each of the 10 low-frequency harmonics is introduced (4th iteration shown overlaid with ○ symbol); (b) absolute magnitudes of the total 128 response harmonics and (c) stable periodic solution compared with starting single harmonic.

3.3.1. The benefits of the SF-HBM

There are three marked advantages with the SF-HBM. The first major advantage of the method is that the total number of harmonics included in the solution is determined by the chosen discrete time interval. This remains fixed, and can be very large from the start, as needed to obtain a fully converged solution. By contrast, only a small number of algebraic equations need to be solved to obtain the total solution. In practice, this starts from three equations, rising typically to no more than about 13 equations as the iteration proceeds. But the total solution may if needed, involve 10's or even 100's of harmonics from the start. This ability to carry a sufficient number of harmonics in the total solution (without the computational burden of having to solve a large system of algebraic equations) overcomes one of the limitations often quoted of the HBM. This first advantage is evident for multi-harmonic forcing, where a large number of solution harmonics are needed. It has been demonstrated that the method only needs to solve algebraic equations for the low-frequency harmonics (typically between 4 and 8 equations for the Duffing oscillator test cases). This gives an enormous improvement in efficiency over the conventional HBM where the size of the algebraic system is directly proportional to the number of response harmonics. When more harmonics are needed in the total solution, this can be achieved with the SF-HBM, by increasing the number of discrete time points. It does not necessarily require the number of low-frequency harmonics to be increased. For example in the 12-harmonic forcing test case, only the mean, and 6 low-frequency harmonics were needed, whereas use of $2^8 = 256$ discrete time points, gave a total of 128 response harmonics.

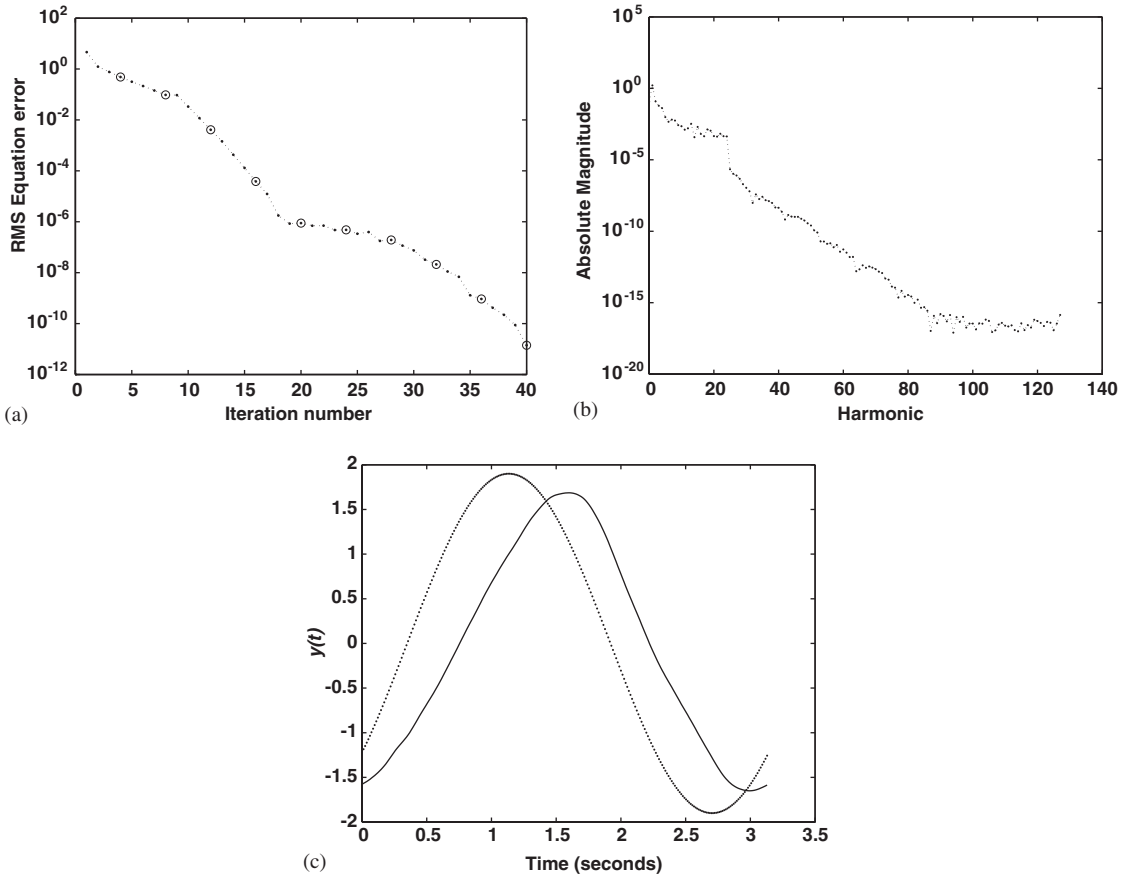

Fig. 17. Solution information at $\Omega/\omega_n = 2$ for oscillator with 7th degree stiffness computed via SF-HBM for 24-harmonic forcing over 256 discrete time points: (a) equation error rms as a function of iteration number (shown as a ● symbol) with four iterations as each of the 10 low-frequency harmonics is introduced (4th iteration shown overlaid with ○ symbol); (b) absolute magnitudes of the total 128 response harmonics and (c) stable periodic solution compared with starting single harmonic.

The second advantage relates to the feasibility of algebraic equation generation and the amount of time involved in practice. Since the SF-HBM is implemented numerically, each of the small number of algebraic equations is generated only when needed using the FFT. This considerably simplifies the construction of the algebraic equations even for expansible nonlinearities (such as quadratic and cubic terms [14,20]) whose manipulation actually makes error elimination difficult. Alternatively, to totally avoid errors arising when handling expansible nonlinearities, symbolic computation can be used in a conventional HBM. But as Fig. 13 shows, the symbolic computation time needed for a cubic nonlinearity is highly dependent on the size of the algebraic system. This burden clearly poses a serious practical limitation on the use of symbolic computation for equation generation with expansible nonlinearities. For non-expansible nonlinearities, it is practically impossible to construct the algebraic equations in closed-form. This means that algebraic equation generation then has to be achieved wholly numerically (i.e. the HBM essentially becomes a Galerkin-type Weighted Residual method). The SF-HBM handles this numerical generation very efficiently via the FFT and therefore, as demonstrated in the paper, has the advantage that non-expansible nonlinearities can be handled efficiently.

A third advantage is that convergence of a solution is confirmed directly in terms of the magnitude of the equation error rather than by the magnitude of the terms neglected. If a method has the ability to converge, then the equation error should approach zero. A very small equation error is clearly not needed in most practical problems but it does indeed confirm that a scheme converges to an accurate solution.

A disadvantage of the proposed SF-HBM is the dependence of successful convergence on a reasonably good initial choice for the starting amplitude and phase of the fundamental harmonic component. The starting

phase in particular, should be in the vicinity of the phase of the fundamental component of the final solution. If the starting choice is poor, then the iterative scheme may fail to converge. When convergence does not occur, it may be difficult to establish whether the problem is one of poor starting values or a non-existent solution. But this problem also occurs with the HBM in general.

4. Conclusions

Nonlinear oscillator responses to multi-harmonic forcing can be obtained using the HBM but as the paper shows, this generally requires correspondingly more response harmonics in the solution than for single-harmonic forcing. This even includes the addition of a small but nonzero mean value response, which unlike single-harmonic forcing, results in a small loss of symmetry. A new SF-HBM has been developed and tested on nonlinear oscillators with multi-harmonic forcing, and shown to give greatly improved accuracy and efficiency compared with a conventional HBM. Test results are obtained for the periodic response at the fundamental driving frequency, resulting from multi-harmonic forcing in the range 1–24-harmonics. To totally avoid errors from entering the algebraic equation generation in a conventional HBM applied to a Duffing model, symbolic computation has been used throughout. The paper shows that a practical limit is imposed by the amount of symbolic computation time needed, even for manipulating expansible nonlinearities, such as a cubic term. The main findings of the paper are that this new SF-HBM offers the following marked benefits:

By splitting the response into nominally low-frequency and nominally high-frequency components, and by writing the equation error in terms of two well-defined functions, a high bandwidth solution (involving 2^{N-1} harmonics) can be obtained by iteration. This involves solving a much smaller system of algebraic equations (for the low-frequency harmonic coefficients) and by obtaining the high frequency coefficients in a separate step.

The small system of algebraic equations associated with the low-frequency harmonics can be very efficiently constructed via the FFT (over 2^N discrete-time intervals per cycle), and solved to very high accuracy using a conventional least square solver. This capability allows oscillators with non-expansible nonlinearities and multi-harmonic forcing to be handled efficiently.

References

[1] A.H. Nayfeh, D.T. Mook, *Nonlinear Oscillations*, Wiley Classics Library Edition, 1995.
[2] P. Malatkar, A.H. Nayfeh, Calculation of the jump frequencies in the response of s.d.o.f. non-linear systems, *Journal of Sound and Vibration* 254 (5) (2002) 1005–1011.
[3] S.L. Lau, Y.K. Cheung, Amplitude incremental variational principle for nonlinear vibration of elastic systems, *Journal of Applied Mechanics* 48 (1981) 959–964.
[4] Y.K. Cheung, S.L. Lau, Incremental time-space finite strip method for nonlinear structural vibration, *Earthquake Engineering and Structural Dynamics* 10 (1982) 239–253.
[5] S.L. Lau, Y.K. Cheung, S.Y. Wu, Incremental harmonic balance method with multiple time scales for aperiodic vibration of nonlinear systems, *Journal of Applied Mechanics* 50 (1983) 871–876.
[6] W. Szemplinska-Stupnicka, Secondary resonances and approximate models of routes to chaotic motion in non-linear oscillators, *Journal of Sound and Vibration* 113 (1) (1987) 155–172.
[7] M.N. Hamdan, T.D. Burton, On the steady state response and stability of non-linear oscillators using harmonic balance, *Journal of Sound and Vibration* 166 (2) (1993) 255–266.
[8] M.I. Friswell, J.E.T. Penny, The accuracy of jump frequencies in series solutions of the response of a Duffing oscillator, *Journal of Sound and Vibration* 169 (1994) 261–269.
[9] K. Worden, On jump frequencies in the response of the Duffing oscillator, *Journal of Sound and Vibration* 198 (1996) 522–525.
[10] S. Sensoy, K. Huseyin, On the application of IHB technique to the analysis of non-linear oscillations and bifurcations, *Journal of Sound and Vibration* 215 (1) (1998) 35–46.
[11] R. Haiwu, X. Wei, M. Guang, F. Tong, Response of a Duffing oscillator to combined deterministic and random excitation, *Journal of Sound and Vibration* 242 (2) (2001) 362–368.
[12] Y.X. Xu, W.B. Bao, W. Schiehlen, H.Y. Hu, A 1/3 pure subharmonic solution and transient process for the Duffing's equation, *Applied Mathematics and Mechanics* 22 (5) (2001) 586–592.
[13] S. Narayanan, K. Jayaraman, Chaotic oscillations of a square prism in fluid flow, *Journal of Sound and Vibration* 166 (1) (1993) 87–101.

[14] I. Senjanović, Harmonic analysis of nonlinear oscillations of cubic dynamical systems, *Journal of Ship Research* 38 (3) (1994) 225–238.
[15] J.C. Peyton Jones, I. Çankaya, Generalised harmonic analysis of nonlinear ship roll dynamics, *Journal of Ship Research* 40 (4) (1996) 316–325.
[16] J.C. Peyton Jones, I. Çankaya, Polyharmonic balance analysis of nonlinear ship roll response, *Nonlinear Dynamics* 35 (2004) 123–146.
[17] G. von Groll, D.J. Ewins, The harmonic balance method with arc-length continuation in rotor/stator contact problems, *Journal of Sound and Vibration* 241 (2001) 223–233.
[18] B.Y. Moon, B.S. Kang, B.S. Kim, Dynamic analysis of harmonically excited non-linear structure system using harmonic balance method, *KMSE International Journal* 15 (11) (2001) 1507–1516.
[19] E.P. Petrov, D.J. Ewins, Analytical formulation of friction interface for analysis of nonlinear multi-harmonic vibrations of bladed disks, *Transactions of the ASME* 125 (2003) 364–371.
[20] A. Raghothama, S. Narayanan, Periodic response and chaos in nonlinear systems with parametric excitation and time delay, *Nonlinear dynamics* 27 (2002) 341–365.
[21] A. Al-shyyab, A. Kahraman, Nonlinear dynamic analysis of a multi-mesh gear train using multi-term harmonic balance method: sub-harmonic motions, *Journal of Sound and Vibration* 279 (2005) 417–451.
[22] L.O. Chua, A. Ushida, Algorithms for computing almost periodic steady-state response of nonlinear systems to multiple input frequencies, *Transactions on Circuits and Systems CAS* 28 (10) (1981) 953971.
[23] J. Driesen, K. Hameyer, Frequency domain finite element approximations for saturable electrical machines under harmonic driving conditions, *International Journal for Computation and Mathematics in Electrical and Electronic Engineering* 19 (2) (2000) 420–425.
[24] R.E. Mickens, Iteration procedure for determining approximate solutions to nonlinear oscillator equations, *Journal of Sound and Vibration* 116 (1987) 185–187.
[25] C.W. Lim, B.S. Wu, A modified Mickens procedure for certain nonlinear oscillations, *Journal of Sound and Vibration* 257 (2002) 202–206.
[26] R.E. Mickens, A generalised iteration procedure for calculating approximations to periodic solutions of "truly nonlinear oscillations", *Journal of Sound and Vibration* 287 (2005) 1045–1051.
[27] R.C. Maple, P.I. King, P.D. Orkwis, J.M. Wolff, Adaptive harmonic balance method for nonlinear time-periodic flows, *Journal of Computational Physics* 193 (2004) 620–641.